








Spatial distribution models and biodiversity of phytoplankton cysts in the Black Sea

Nina Dzhebekova^{1*}, Ivelina Zlateva^{1*}, Fernando Rubino², Manuela Belmonte², Valentina Doncheva¹, Ivan Popov¹, Snejana Moncheva¹

¹ Institute of Oceanology “Fridtjof Nansen” – Bulgarian Academy of Sciences, Parvi May 40, Varna, Bulgaria

² Water Research Institute, National Research Council (CNR-IRSA), Via Roma, 3, 74123 Taranto, Italy

Corresponding author: Ivelina Zlateva (ibikarska@yahoo.com)

This article is part of:

Black Sea ecosystem in the spotlight

Edited by Kremena Stefanova,
Snejana Moncheva, Ertuğ Düzgüneş,
Lyubomir Dimitrov



Academic editor: Kremena Stefanova

Received: 19 February 2024

Accepted: 26 April 2024

Published: 4 June 2024

ZooBank: <https://zoobank.org/482438F8-1416-4909-B405-53CAD98C8ED4>

Citation: Dzhebekova N, Zlateva I, Rubino F, Belmonte M, Doncheva V, Popov I, Moncheva S (2024) Spatial distribution models and biodiversity of phytoplankton cysts in the Black Sea. *Nature Conservation* 55: 269–296. <https://doi.org/10.3897/natureconservation.55.121181>

Copyright: © Nina Dzhebekova et al.
This is an open access article distributed under terms of the Creative Commons Attribution License (Attribution 4.0 International – CC BY 4.0).

Abstract

The current study employed diverse statistical and machine learning techniques to investigate the biodiversity and spatial distribution of phytoplankton cysts in the Black Sea. The MaxEnt distribution modeling technique was used to forecast the habitat suitability for the cysts of three potentially toxic microalgal taxa (*Lingulodinium polyedra*, *Polykrikos hartmannii*, and *Alexandrium* spp.). The key variables controlling the habitat suitability of *Alexandrium* spp. and *L. polyedra* were nitrates and temperature, while for the *P. hartmannii* cysts, nitrates and salinity. The region with the highest likelihood of *L. polyedra* cyst occurrence appears to be in the western coastal and shelf waters, which coincides with the areas where *L. polyedra* red tides have been documented. The projected habitat suitability of the examined species partially overlapped, perhaps as a result of their cohabitation within the phytoplankton community and shared preferences for specific environmental conditions, demonstrating similar survival strategies. The north-western region of the Black Sea was found to be the most suitable environment for the studied potentially toxic species, presumably posing a greater risk for the onset of blooming events. Two distinct aspects of cysts' ecology and settlement were observed: the dispersal of cysts concerns their movement within the water column from one place to another prior to settling, while habitat suitability pertains to the particular environment required for their survival, growth, and germination. Therefore, it is crucial to validate the model in order to accurately determine a suitable habitat as well as understand the transportation patterns linked to the particular hydrodynamic properties of the water column and the distinct features of the local environment.

Key words: Black Sea, cyst assemblages, habitat suitability, harmful algal blooms, MaxEnt, potentially toxic phytoplankton

Introduction

As essential primary producers, phytoplankton biodiversity has a profound ecological impact on the state and dynamics of marine ecosystems and can influence their functioning via global biogeochemical cycling of carbon, nitrogen, phosphorus, and silicate, in addition to primary productivity (Ptacnik et al.

* These authors have contributed equally to this work.

2008; Ellegaard and Ribeiro 2018). A considerable number of phytoplankton species undergo benthic dormant phases throughout their life cycles (Belmonte and Rubino 2019). These dormant stages may result from either sexual reproduction, such as the resting cysts of dinoflagellates and the resting spores of some diatoms, or vegetative division, such as the resting spores or resting cells of most diatoms (Ellegaard and Ribeiro 2018). Some of the species forming benthic resting stages may produce harmful algal blooms, which can have detrimental impacts on the environment and result in substantial economic losses (Hallegraeff 1993). Phytoplankton cysts that have accumulated in sediments may remain viable for several decades or potentially up to a century (Lundholm et al. 2011), serving as potential seed banks, maintaining biodiversity over time (Kremp et al. 2018), and contributing to bloom dynamics (Lundholm et al. 2011; Anderson et al. 2014; Castañeda-Quezada et al. 2021). Therefore, benthic seed banks hold significant ecological importance by playing a vital role in enhancing the resilience of phytoplankton populations, particularly in changing environments (Picoche and Barraquand 2022). Dinoflagellate cysts have been extensively utilized as a proxy for studying alterations in sea-surface conditions (Sgrosso et al. 2001; Godhe and McQuoid 2003; Pospelova et al. 2004; Richter et al. 2007; Kremp et al. 2009; Zonneveld et al. 2013; Mudie et al. 2017; Shin et al. 2018). Given the discontinuous presence of phytoplankton species in the water column (Lundholm et al. 2011), studying the structure and distribution of cysts' communities can provide important insights into the diversity of phytoplankton (specifically those that form cysts) over time, environmental shifts, and potential harmful algal blooms associated with cysts (Mudie et al. 2017). The latter could have major implications for vulnerable ecosystems such as the Black Sea, which is characterized by its high level of isolation from the global ocean, substantial inflow of freshwater, pronounced vertical stratification, low salinity, and elevated concentrations of hydrogen sulfide below depths of 150–200 meters.

The composition and survival of cyst assemblages in pelagic communities rely heavily on the species' distinct morphological, biochemical, and physiological characteristics, as well as the fluctuations in biological, physical, and chemical oceanographic conditions in both surface water and bottom sediments (Ellegaard and Ribeiro 2018 and the references therein). The Atlas of modern dinoflagellate cyst distributions in the Black Sea Corridor (Mudie et al. 2017) provides a thorough reference for enhancing our knowledge of the connections between surface water conditions and the distribution, diversity, and morphological variations of dinoflagellate cysts in the Black Sea. Additional research on cyst assemblages and their correlation with environmental variables may aid in the evaluation and modeling of the distinct distribution patterns of cysts in sediments, as well as in the expansion of our knowledge of these complex interactions. This is particularly essential for the mapping of cyst banks containing potentially harmful/toxic species.

Spatial distribution modeling (SDM) has gained significant recognition in recent years as a highly effective method for assessing the spatial status of biodiversity (Cayuela et al. 2009). It is widely acknowledged as an accurate approach for identifying the habitat preferences of species in response to certain environmental variables (Guisan and Thuiller 2005). SDMs are predictive

models that utilize the spatial distribution of documented species occurrences and analyze them in relation to different environmental factors. This analysis is facilitated through the use of statistical algorithms that aim to elucidate the influence of the environment on the patterns of species presence or absence (Guisan and Thuiller 2005; Coops et al. 2009; Elith and Leathwick 2009). The present research employed the Maximum Entropy (MaxEnt) modeling technique. The latter refers to a machine learning algorithm that has been specifically designed to make predictions using incomplete data (Baldwin 2009). The method is to determine the sampling sites' distribution that is the most uniform in comparison to the background locations, taking into account the constraints related to the data. The maximum entropy algorithm is a deterministic approach that exhibits convergence towards the probability distribution with the highest entropy (Baldwin 2009). Hence, the resultant output indicates the degree to which the model presents a more precise alignment with the location data in comparison to a uniform distribution. The MaxEnt algorithm has several advantages, one of the most notable being its capability to model both continuous and categorical variables. In addition, MaxEnt performs variable transformation and feature selection, maximum entropy model fitting, and regularization techniques in order to avoid the likelihood of model overfitting. Furthermore, the output generated by the model is rather easy to interpret. The predictive accuracy of MaxEnt has consistently demonstrated comparability to the most efficient modeling techniques, and it has been successfully employed to model the biogeographic distributions of species in various regions of the world (Yost et al. 2008; Elith et al. 2011; Smith et al. 2012; White et al. 2012; Urbani et al. 2015; Mamun et al. 2018; Wang et al. 2018; Holder et al. 2020; Yan et al. 2020).

In this study, the biodiversity of modern cyst assemblages was examined in sediment samples collected from 30 sites (coastal and shelf) in the Black Sea. The species composition, abundance, diversity indices, and association of species with sites and sediment types were analyzed. The MaxEnt distribution modeling technique was employed to accurately fit habitat suitability models for the distribution of cysts of three potentially toxic microalgal taxa (*Lingulodinium polyedra*, *Polykrikos hartmannii*, and *Alexandrium* spp.) in the Black Sea basin. The objective was to evaluate the extent to which their distribution is influenced by specific environmental variables.

Methods

Sampling

The study region encompassed the Black Sea waters of Bulgaria (BG), Romania (RO), Ukraine (UA), Georgia (GE), and Turkey (TR) (Fig. 1, Suppl. material 1: table S1). A total of 47 surface sediment samples (top 2 cm) were collected at 30 sites, ranging in depth from 7.5 to 101 meters. These samples were obtained throughout various campaigns conducted between April 2008 and June 2016, primarily in the spring and/or summer seasons. The collection methods used either a multicorer or a Van Veen Grab sampler. The sediment samples were stored in a light-free environment at a temperature of 4 °C without any preservatives until they were processed.

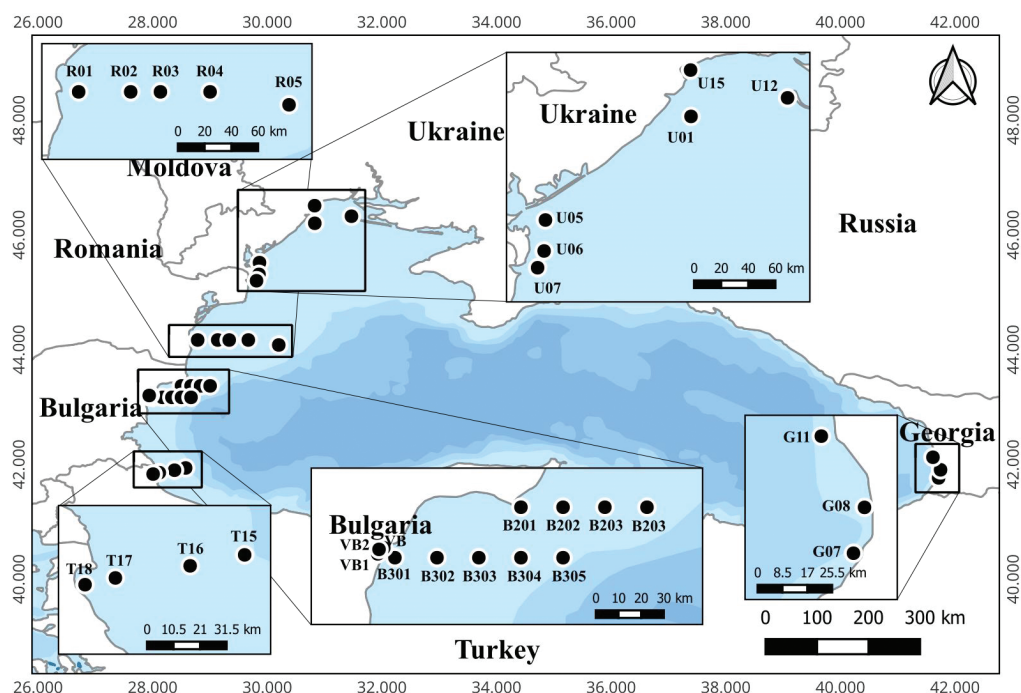


Figure 1. Map of sampling sites and locations of stations in the Black Sea.

Sediment treatment, qualitative, and quantitative analysis of cysts

An aliquot of homogenized sediment (from 2.0 to 2.2 cm³) was taken from each sample for cyst analysis. Additionally, a separate aliquot (≈ 10 cm³) was obtained to determine the water content. The wet aliquots were weighed and screened through a 10 μ m mesh (Endecotts Limited steel sieves, ISO3310-1, London, England) using natural filtered (0.45 μ m) seawater (Montresor et al. 2010). The material retained on the sieve was ultrasonicated for 1 min at low frequency and screened again through a sieve battery (200, 75, and 20 μ m mesh sizes). A fine-grained fraction (20–75 μ m), mainly containing protistan cysts, was obtained. The material retained on the 75 and 200 μ m mesh was not considered in this study. No chemicals were used to dissolve sediment particles in order to preserve calcareous and siliceous cyst walls.

Qualitative and quantitative analyses were carried out under an inverted microscope (Zeiss Axiovert 200M) equipped with a Leica MC170 HD digital camera at $\times 320$ –400 magnification. Both full cysts with cytoplasmic content (i.e., presumably viable) and empty, already germinated cysts were enumerated, but the empty cysts were not considered in this study; a minimum of 200 viable cysts were counted for each sample to obtain abundance values as homogeneous as possible and evaluate rare species too.

To estimate the water content of sediment, an aliquot from each sample (≈ 10 cm³) was weighed and dried out at 70 °C. Quantitative data are reported as cysts per gram of dry sediment (cysts g⁻¹). The results from the repetitive stations (which were sampled more than once for the study period in separate expeditions) were compiled, and the highest abundance values were utilized for the analyses.

All resting-stage morphotypes were identified using previously published descriptions. The organic dinocysts were analyzed using the images and keys supplied in Mudie et al. (2017). The currently accepted biological taxonomic (motile-cell) names were used preferentially according to WoRMS (2023).

Statistical analyses

Biodiversity indices were utilized to conduct a robust evaluation of the distinct patterns and preferences of species with regard to habitat or site groups. This included assessing the species richness per habitat/sediment type, examining the association between species and habitat/sediment type, and determining the effectiveness of species as indicators of site groups. The habitat types were defined according to Vasquez et al. (2021). The analyses were performed using the R environment version 4.1.2 (R Core Team 2022), utilizing the 'BiodiversityR' package (Kindt and Kindt 2019) and the 'indicpecies' package (De Cáceres and Jansen 2016).

In addition, the present study examined the spatial distribution of cyst assemblages of three potentially toxic taxa, specifically *L. polyedra*, *P. hartmanii*, and *Alexandrium* spp., utilizing the Maximum Entropy machine learning algorithm. The models were initially fitted and cross-validated using MaxEnt software Version 3.4.4 (Phillips et al. 2017) and thereafter developed in the Jupiter Notebook environment (Kluyver et al. 2016) using the Python programming language (Van Rossum and Drake 1995) version 3.9.0 through the implementation of elapid-species distribution modeling tools for Python (Anderson 2023) that offer a customized implementation of the Maximum Entropy machine learning modeling technique and a collection of methods for analyzing biogeography data. It enables the incorporation of spatial components into the model through features such as sample weighting and geographic k-fold cross-validation. Elapid enhances user control and comprehension of the complex MaxEnt approach, thereby improving flexibility. Consequently, this assists users with developing and evaluating their models more effectively. The latter facilitates the process of modeling data that varies over time across multiple scales, fitting models that consider geographic weighting, creating ensembles of models, accurately defining the distribution of background points, and summarizing the predictions made by the model.

The input data for the MaxEnt model includes a collection of species' presence-only (PO) locations and a set of environmental predictors within a spatial extent selected by the user. The MaxEnt algorithm selects a set of background locations, which are then compared to the known presence locations. Based on this comparison, MaxEnt produces an estimation of the probability of species presence or relative environmental suitability. This estimation ranges from 0 (indicating the least likelihood) to 1 (indicating the most likelihood) (Phillips et al. 2006, 2017).

Species data were compiled by using the present sampling data and additional published data (Mudie et al. 2017) for potentially toxic taxa cyst assemblages of interest (*P. hartmanii*, *L. polyedra*, and *Alexandrium* spp.), considering only sampling stations at depths up to 200 m, encompassing the coastal and shelf waters (0–200 m) of the Black Sea basin. As a result, the species datasets were constructed by taking into consideration the PO locations: 72 records for *Alexandrium* spp. cyst occurrence in sediment samples, 80 PO records for *L. polyedra*, and 38 records for *P. hartmanii*.

Furthermore, another suite of Python libraries commonly employed for data processing and visualization was utilized: the GDAL/OGR library (GDAL/OGR contributors 2022), numpy (Harris et al. 2020), rasterio (Gillies 2019), sklearn (Pedregosa et al. 2011), pandas (McKinney 2010), geopandas (Jordahl et al.

2020), matplotlib (Ari and Ustazhanov 2014), shapely (Gillies 2013), xarray (Hoyer and Hamman 2017), and cmocean (Thyng et al. 2016). The properties of the water column were studied in a Python programming environment through the use of the GSW Oceanographic Toolbox, the version developed for Phyton (McDougall and Barker 2011).

Environmental variable selection

The selection of abiotic factors as predictors was based on previous research into the extent of their influence and ecological principles concerning species preferences for habitat, as well as their impact on the variability of phytoplankton biomass. The variables of interest include surface sea temperature, salinity, current velocities, concentrations of chlorophyll *a* and dissolved oxygen, as well as pH levels, phosphates, and nitrate concentrations in seawater, proven as primary factors affecting benthic cyst assemblages (Godhe and McQuoid 2003; Ribeiro and Amorim 2008; Mudie et al. 2017; Li et al. 2019; García-Moreiras et al. 2021). The suite of selected predictor variables was processed as digital layers to be utilized when fitting the models. While it was expected that some of the chosen predictors might be correlated, the maximum entropy algorithms used in training the model are robust to collinearity among predictors. MaxEnt also accounts for redundant variables through regularization implementation (Feng et al. 2019). Therefore, the initial exclusion of highly correlated variables through feature dimension reduction methods had minimal impact on improving the model. Considering the latter, the initial set of predictor variables was retained.

The Copernicus Marine Environmental Service (CMEMS) data portal, accessed on 20 December 2023, was used to acquire monthly mean environmental data layers for the selected variables spanning from 1993 to 2016. These data layers correspond to the sampling expeditions and additional published data (Mudie et al. 2017) that were employed to compile the final datasets of species-presence-only (PO) localities.

CMEMS data were produced by numerical simulation models that combine in situ and satellite data for the Black Sea profile. The models used are the hydrodynamic NEMO (Nucleus for European Modeling of the Ocean) and the BAMHBI (Biogeochemical Model for Hypoxic and Benthic Influenced Areas) (Grégoire et al. 2008; Grégoire and Soetaert 2010; Capet et al. 2016). The data were constructed by utilizing two products: The Black Sea Physics Reanalysis (Lima et al. 2020), covering the time span from 1993 to 2016, with a spatial resolution of $0.037^\circ \times 0.028^\circ$, and the Black Sea Biogeochemistry Reanalysis (Grégoire et al. 2020). The latter offers monthly climatology fields for the specified time period, with a spatial resolution of $0.025^\circ \times 0.025^\circ$.

The datasets were averaged over the study period using MATLAB (The Math Works, Inc. MATLAB, version 2020a) for the Black Sea region. The original spatial resolution was maintained for the data obtained from the Black Sea Biogeochemistry Reanalysis, while the data obtained from the Black Sea Physics Reanalysis were resampled from $0.037^\circ \times 0.028^\circ$ to a denser resolution of $0.025^\circ \times 0.025^\circ$. The data for each layer was extracted in ESRI ASCII grid format (subsequent conversion to GeoTIFF data format took place in the maximum entropy models' implementation in Python).

Model evaluation and validation

The resultant SDMs were cross-validated with ten replicate model runs in MaxEnt and checkerboard geographic structuring in the Python implementation for an adequate evaluation of their performance. Additionally, 25% of PO data was set aside to be utilized as a randomly selected test sample for every model run in MaxEnt and 50% in the Python implementation. Checkerboard partitions provide an effective solution by implementing geographical structuring and masking at the finer level, henceforth minimizing spatial correlation between training and testing data (Pearson et al. 2013; Muscarella et al. 2014; Anderson 2023).

The performance of the resulting SDMs was assessed using the area under the curve (AUC) of receiver operating characteristic (ROC) metrics (Fielding and Bell 1997), and additionally, the model accuracy score and the misclassification rate were evaluated for the Python implementation of the models. Both metrics (AUC and accuracy) are being used to evaluate SDM performance; nevertheless, they capture different aspects of model performance. AUC metrics measure the model's ability to discriminate between positive and negative instances, while accuracy measures the overall correctness of predictions (Hossin and Sulaiman 2015). Conversely, the misclassification rate, which is equal to 1 minus the accuracy (*misclassification rate* = 1 – *accuracy score*), is a measure of the likelihood of misclassification based on the model's predictions (Bekkar et al. 2013).

Additionally, the stability of the water column was studied through the Python implementation (McDougall and Barker 2011) of the Gibbs SeaWater (GSW) Oceanographic Toolbox of TEOS-10 (IOC, SCOR, and IAPSO 2010) to address the specifics of the hydrodynamic conditions and cyst transportation patterns. Considering the latter, the in situ density of the water column $\rho = \hat{\rho}(S_A, \Theta, p)$ was calculated for the whole spatial extent along the depth gradient (31 depth levels) as a function of absolute salinity (S_A) conservative temperature (Θ), and pressure (p) using the 75-term expression implemented in GSW toolbox functions (Roquet et al. 2015). The absolute salinity S_A was derived by the practical salinity S through the conversion functions available in the toolbox, and the conservative temperature (Θ) (ITS-90) by the potential temperatures θ and S_A , using the computationally efficient expression for specific volume in terms of S_A , Θ , and p (Roquet et al. 2015). The vertical stability of the water column over the latitudinal gradient was examined by the Brunt-Vaisala (buoyancy) frequency: $N^2 = g^2 \rho \frac{\beta^\Theta \Delta S_A - \alpha^\Theta \Delta \Theta}{\Delta P}$, where ΔS_A and $\Delta \Theta$ are the differences between the absolute salinities and conservative temperatures of vertically adjacent seawater parcels separated by pressure ΔP measured in Pa. The density and the saline concentrations, including the thermal expansion coefficients β^Θ and α^Θ , were evaluated at the average values of S_A , Θ , and p by using the functions implemented in the GSW toolbox (IOC, SCOR, and IAPSO 2010; Roquet et al. 2015). The Turner angle Tu and the stability ratio R_p of the water column were evaluated using the 75-term expression $\hat{v}(S_A, \Theta, p)$, implemented in GSW toolbox functions (IOC, SCOR, and IAPSO 2010; Roquet et al. 2015).

All maps and graphs were created using QGIS version 3.34 (QGIS Development Team 2009) and the Python library Matplotlib (Ari and Ustazhanov 2014).

Results

Species Composition and Abundance of Resting Stages in Sediments

The assemblages of phytoplankton resting stages discovered in the sediments of the Black Sea were highly diverse, consisting of a total of 71 distinct taxa, with 41 identified at the species level. These taxa were classified into 23 genera, which belonged to six orders and two classes (Table 1). Furthermore, 15 uncertain dinoflagellate taxa and six species described as fossils whose active stage is not known were determined in the samples but excluded from the analyses. The majority of the detected taxa belonged to Dinophyceae (91.5%), and only 8.5% were representatives of Bacillariophyceae. The highest taxonomic diversity (including several unidentified species-level taxa differentiating in form and size) was observed within the genera *Scrippsiella* (13 taxa), *Alexandrium* (13 taxa), and *Protoperidinium* (11 taxa).

Overall, the distribution of most species in the studied area was not uniform. The most prevalent taxa, detected at 70% or more of the stations, were *Scrippsiella acuminata* (found at all stations), followed by *Scrippsiella* sp. 1, *Pentapharsodinium tyrrhenicum*, *Pentapharsodinium dalei*, *Lingulodinium polyedra*, *Gonyaulax* sp., *Protoperidinium* sp. 1, *Scrippsiella* sp. 5, *Calciodinellum albatrosianum*, *Scrippsiella* sp. 4, and *Chaetoceros* sp. 1. A total of 17 additional taxa, on the contrary, were recorded as a single entry.

Considerable spatial variability in total cyst concentration has been observed, ranging between 5 cysts g⁻¹ (st. VB and B202/June 2008) and 11,929 cysts g⁻¹ (st. B305/July 2013) (Suppl. material 1: table S2). The most abundant taxa, in terms of relative abundance, were the diatom resting stages of *Chaetoceros* sp. 1, which made up over 40% of the total cyst count in 13 samples, and *Chaetoceros* sp. 2, which accounted for up to 28% of the total cyst count in one sample. Additionally, *Scrippsiella acuminata* dinoflagellate cysts were present in relative abundance, ranging from 10% to 100%; *Scrippsiella* sp. 1 cysts presented between 12% and 33% in 13 samples; and *Lingulodinium polyedra* cysts were between 12% and 25% in 4 samples. The diatom species *Chaetoceros* sp. 1 and *Chaetoceros* sp. 2 had the highest concentrations of 6793 cysts g⁻¹ and 1598 cysts g⁻¹ at station B305 in July 2013. The dominant dinoflagellates *Scrippsiella acuminata*, *Lingulodinium polyedra*, and *Scrippsiella* sp. 1 had the highest concentrations at station U01 in May 2016, with 2741 cysts g⁻¹, 1722 cysts g⁻¹, and 1463 cysts g⁻¹, respectively. The diatom resting stages of *Chaetoceros* sp. 2 were quite abundant (exhibiting peaks in certain samples); however, their occurrence was sporadic, being found at only 7 sites. In contrast, several common taxa (*Calciodinellum albatrosianum*, *Gonyaulax* sp., *Pentapharsodinium dalei*, *Protoperidinium* sp. 1, *Pentapharsodinium tyrrhenicum*, *Scrippsiella* sp. 4, and *Scrippsiella* sp. 5) found in over 57% of the samples, despite being present in a wide range of cyst reservoirs, do not reach high abundances, with the highest concentrations being less than 190 cysts g⁻¹.

Out of the resting stages that were detected, eight types were assigned to potentially toxic microalgae species: *Alexandrium minutum*, *A. pseudogonyaulax*, *A. tamarense*, *A. taylorii*, *Gonyaulax spinifera*, *Lingulodinium polyedra*, *Polykrikos hartmannii*, and *Protoceratium reticulatum*. The cysts of these potentially toxic dinoflagellates, except for *L. polyedra*, were in low abundance, with the highest

concentrations not exceeding 81 cysts g⁻¹. The majority of the species exhibited sporadic distribution, being present in just 2–23% of the samples (3–33% of the sampling stations). However, *Polykrikos hartmannii* and *Alexandrium minutum* were more widespread, being detected in 40% and 49% of the samples and 50% and 60% of the stations, respectively.

Diversity indices and species association to sites and sediment type

The species richness detected at each station exhibited significant variability (Suppl. material 1: table S3), ranging from 2 (st. VB) to 45 (st. B305), with just one species, *Scrippsiella acuminata*, consistently present in the cyst assemblages. The Shannon diversity index (H) varied between 0.41 (st. G11) and 2.05 (st. U06) (Suppl. material 1: table S3). The highest values (> 1.89) were calculated for the Ukrainian coastal stations (U06, U05, U15, and U12). The stations exhibiting the lowest diversity indices were G11 (H = 0.41) and VB (H = 0.45), mostly due to the dominant presence of *Scrippsiella acuminata* and *Scrippsiella* sp. 1, which accounted for 91% of the overall abundance at both stations. The lower values of Pielou's evenness index (J), ranging between 0.21 (st. G11) and 0.71 (st. B204), in 80% below 0.6 (Suppl. material 1: table S3), indicated the dominance of specific taxa in the cyst assemblages.

The species richness per sediment type showed a high degree of similarity, with an average of 9.7 ± 0.4 species per sediment type. Additionally, the Fishers' alpha diversity index values were comparable across all five sediment types, ranging from 1.256 (sand) to 1.596 (muddy sand) (Suppl. material 1: table S4). The beta diversity displayed a range of values from 0 ("Muddy sand") to 0.418 ("Fine mud"), with an average of 0.234.

The indicator species analysis displayed a statistically significant association between specific sediment types and cyst species (Suppl. material 1: table S5). Eight species were associated with the group (sediment type) "muddy sand" (*Chaetoceros* sp. 3, *Chaetoceros* sp. 6, *Protoperidinium* sp. 9, *Diplopsalis* sp., *Protoperidinium claudicans*, *Protoperidinium* sp. 6, *Alexandrium margalefii*, and *Pyrophacus horologium*), whereas one species (*Alexandrium tamarense*) was associated with the group "mixed sediment + muddy sand." The remaining types of sediments showed low indicator values (*ind val*) and no statistically significant results; hence, no associated species were detected.

A statistically significant association was found between certain site groupings (areas) and certain cyst species (Suppl. material 1: table S6). Three species (*Protoperidinium* sp. 9, *Scrippsiella kirschiae*, and *Scrippsiella* sp. 2) were indicative for the Bulgarian sites, six species (*Alexandrium margalefii*, *Alexandrium pseudogonyaulax*, *Calciadinellum albatrosianum*, *Oblea rotunda*, *Scrippsiella lachrymosa*, and *Scrippsiella* sp. 8) were associated to Romanian sites, three species (*Alexandrium taylorii*, *Archaeperidinium minutum*, and *Scrippsiella* sp. 9) were indicator species for Turkish sites, and 13 species (*Alexandrium* sp. 10, *Alexandrium* sp. 4, *Alexandrium* sp. 7, *Chaetoceros* sp. 4, *Diplopsalis lenticula*, *Dissodinium pseudocalani*, *Ensiculifera carinata*, *Gymnodinium impudicum*, *Levanderina fissa*, *Lingulodinium polyedra*, *Pentapharsodinium dalei*, *Scrippsiella* sp. 1, and *Scrippsiella* sp. 5) were related to Ukrainian sites. No indicator species were found for the Georgian site group.

Table 1. Cyst species identified in the samples and number of stations (%) within different geographic locations. In the table, the different cyst types unidentified at the species level were pooled as spp. and their types noted in brackets. (* potentially toxic species; + species not reported in Mudie et al. 2017). The taxonomic nomenclature is according to WoRMs (<https://www.marinespecies.org/>; accessed on 23 April 2024).

Class	Order	Species	% Stations Where Detected				
			BG	RO	UA	GE	TR
Dinophyceae	Gonyaulacales	<i>Alexandrium cf. margalefii</i> Balech, 1994 *	33	100	17	0	100
		<i>Alexandrium cf. taylorii</i> Balech, 1994 **	0	0	0	0	25
		<i>Alexandrium minutum</i> Halim, 1960 **	42	100	67	0	100
		<i>Alexandrium pseudogonyaulax</i> (Biecheler) Horiguchi ex K.Yuki & Y.Fukuyo, 1992 *	25	40	0	0	100
		<i>Alexandrium tamarense</i> (Lebour) Balech, 1995 **	33	80	0	0	50
		<i>Alexandrium</i> spp.(8 different cyst types/species)	8, 8, 8, 25, 0, 17, 0, 8	0	17, 0, 0, 83, 17, 67, 17, 33	67, 0, 0, 33, 0, 33, 0, 0	0, 0, 0, 0, 0, 0, 0, 25
		<i>Gonyaulax</i> sp.	67	100	67	100	100
		<i>Gonyaulax spinifera</i> (Claparède & Lachmann) Diesing, 1866 *	0	40	17	0	50
		<i>Lingulodinium polyedra</i> (F.Stein) J.D.Dodge, 1989 *	67	100	83	67	100
		<i>Protoceratium reticulatum</i> (Claparède & Lachmann) Bütschli, 1885 *	8	20	0	67	25
		<i>Pyrodinium bahamense</i> L.Plate, 1906	17	60	0	0	50
		cf. <i>Pyrophacus horologium</i> F.Stein, 1883 +	17	60	0	0	0
		Gymnodiniales	<i>Gymnodinium cf. litoralis</i> A.Reñé, 2011 +	25	60	33	33
<i>Gymnodinium impudicum</i> (S.Fraga & I.Bravo) Gert Hansen & Moestrup, 2000 +	50		20	67	0	100	
<i>Gymnodinium nolleri</i> M.Ellegaard & Ø.Moestrup, 1999	42		100	83	100	50	
<i>Gymnodinium</i> spp. (4 different cyst types/species)	0, 0, 17, 8		20, 20, 40, 0	0, 0, 17, 0	0	0, 0, 25, 0	
<i>Nematodinium armatum</i> (Dogiel) Kofoid & Swezy, 1921 +	0		0	0	0	25	
<i>Polykrikos hartmannii</i> W.M.Zimmermann, 1930 *	42		80	17	67	75	
<i>Warnowia rosea</i> (Pouchet) Kofoid & Swezy, 1921 +	25		40	0	0	50	
Dinophyceae incertae sedis	<i>Levanderina fissa</i> (Levander) Moestrup, Hakanen, Gert Hansen, Daugbjerg & M.Ellegaard, 2014 +	25	0	17	0	0	
Peridinales	<i>Archaeperidinium minutum</i> (Kofoid) Jørgensen, 1912 +	8	0	0	0	25	
	<i>Calciodinellum albatrosianum</i> (Kamptner) Janofske & Karwath, 2000 +	58	100	67	67	100	
	<i>Diplopelta parva</i> (T.H.Abé) K.Matsuoka, 1988 +	0	0	17	0	0	
	<i>Diplopsalis lenticula</i> Bergh, 1882 +	42	80	83	33	75	
	<i>Diplopsalis</i> sp.	17	0	0	0	0	
	cf. <i>Ensiculifera carinata</i> Matsuoka, Kobayashi & Gains, 1990 +	42	100	83	33	100	
	<i>Kryptoperidinium foliaceum</i> (F.Stein) Lindemann, 1924 +	0	20	50	0	50	
	<i>Oblea rotunda</i> (Lebour) Balech ex Sournia, 1973 +	33	100	50	0	25	
	<i>Pentapharsodinium dalei</i> Indelicato & Loeblich III, 1986	75	100	67	67	100	
	<i>Pentapharsodinium tyrrhenicum</i> (Balech) Montresor, Zingone & Marino, 1993 +	100	100	67	67	100	
	<i>Protoperidinium claudicans</i> (Paulsen, 1907) Balech, 1974	17	40	0	0	0	
	<i>Protoperidinium compressum</i> (Abé) Balech, 1974 +	8	20	0	0	0	
	<i>Protoperidinium conicum</i> (Gran) Balech, 1974	42	100	33	0	25	
	<i>Protoperidinium oblongum</i> (Aurivillius) Parke & Dodge, 1976	25	100	17	0	50	

Class	Order	Species	% Stations Where Detected				
			BG	RO	UA	GE	TR
Dinophyceae	Peridiniales	<i>Protoperidinium parthenopes</i> A.Zingone & M.Montresor, 1988 ⁺	33	60	50	33	50
		<i>Protoperidinium steidingerae</i> Balech, 1979 ⁺	0	0	17	0	0
		<i>Protoperidinium thorianum</i> (Paulsen, 1905) Balech, 1973 ⁺	25	40	0	33	50
		<i>Protoperidinium</i> spp. (4 different cyst types/species)	58, 8, 25, 8	100, 40, 20, 0	100, 33, 0, 0	33, 0, 33, 0	100, 25, 25, 0
		<i>Scrippsiella acuminata</i> (Ehrenberg) Kretschmann, Elbrächter, Zinssmeister, S.Soehner, Kirsch, Kusber & Gottschling, 2015	100	100	100	100	100
		<i>Scrippsiella kirschiae</i> Zinssmeister, S.Soehner, S.Meier & Gottschling, 2012 ⁺	8	0	0	0	0
		<i>Scrippsiella lachrymosa</i> J.Lewis, 1991 ⁺	33	100	0	0	50
		<i>Scrippsiella ramonii</i> M.Montresor, 1995 ⁺	8	0	17	0	0
		<i>Scrippsiella spinifera</i> G.Honsell & M.Cabrini, 1991 ⁺	17	20	0	0	25
		<i>Scrippsiella trifida</i> J.Lewis, 1991	42	40	0	0	50
	<i>Scrippsiella</i> spp.(7 different cyst types/species)	83, 8, 58, 58, 25, 25, 0	100, 0, 100, 80, 40, 40, 0	100, 0, 83, 100, 50, 0, 0	100, 0, 33, 33, 33, 0, 0	100, 25, 75, 100, 100, 25, 25	
Pyrocystales	<i>Dissodinium pseudocalani</i> (Gonnert) Drebes ex Elbrachter & Drebes, 1978 ⁺	25	60	50	0	50	
Bacillariophyceae	Chaetocerotanae incertae sedis	<i>Chaetoceros</i> spp. (6 different cyst types/species)	33, 25, 8, 8, 8, 0	100, 60, 0, 0, 0, 0	100, 0, 0, 17, 0, 0	67, 0, 0, 0, 0, 33	100, 25, 0, 0, 0, 0

SDM and model validation

The grid output of the maximum entropy species distribution models (SDMs) uses a gradient color scale to represent the mean predicted probability (ranging from 0 to 1) of the most suitable habitat for the species being studied. The models produced clear visual representations (Fig. 2A–C) (MaxEnt Version 3.4.4 gridded outputs are shown in Suppl. material 1: fig. S1A–C) that showed a concentrated area with a high likelihood of the species being present, based on its preferred habitat. This area mainly occurred within the depth range of 2.5–100 meters and extended across the entire western coast of the basin. The most distinct distribution patterns were observed on the North-Western shelf. Moreover, the region that exhibits the highest suitability is evidently coincident with each of the studied species.

Model performance evaluation

In general, AUC values ranging from 0.8 to 0.9 are regarded as very good, while values over 0.9 are considered excellent (Peterson et al. 2012) (Table 2). The aforementioned conditions are equally applicable to the accuracy of the model. Caution should be applied when interpreting the AUC and accuracy results for imbalanced sets. However, the objective of the current study was to model habitat suitability rather than anticipate projections under various environmental conditions or introduce novel grounds.

According to MaxEnt outcome on predictor variables contribution to SDMs relative predicted probabilities (Table 3), the mean values of nitrates, temperature, salinity, and phosphates have the highest contribution in modeling the training data. Additionally, the permutational importance of variables was assessed in the SDMs Python implementation, and the variables that had the highest fitting test data were phosphates, temperature, and salinity.

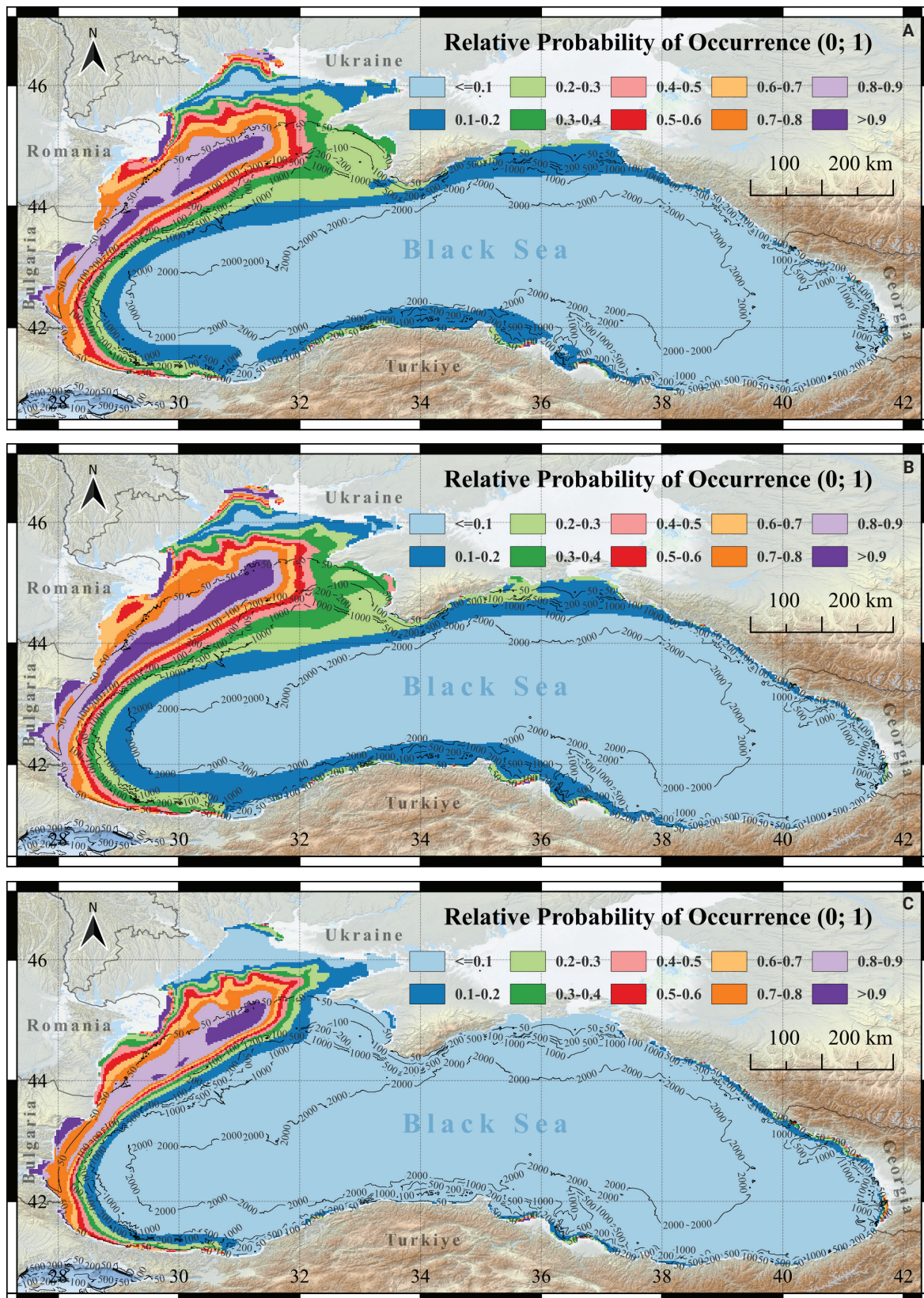


Figure 2. Maximum Entropy Habitat suitability maps (representing the elapid (python implementation tools for SDM) models' outcome) of **A** *Alexandrium* spp. **B** *L. polyedra* **C** *P. hartmanii* in the Black Sea coastal and shelf waters (represented with a color scheme, with light blue indicating the least likelihood of suitable conditions, light orange indicating conditions matching those where species were found, and purple corresponding to the highest predicted probability of a suitable environment).

Table 2. SDM performance evaluation metrics.

		<i>Alexandrium</i> spp.	<i>L. polyedra</i>	<i>P. hartmanii</i>
MaxEnt Version 3.4.4	Avg AUC – replicated SDMs overall performance	0.904±0.056	0.901±0.030	0.920±0.033
Maxent Python Elapid	Unweighted naïve* AUC score – training data	0.935	0.901	0.913
Maxent Python Elapid	Weighted naïve AUC score (training data with samples’ geographic weights)	0.925	0.887	0.989
Maxent Python Elapid	Checkerboard Cross-validation AUC score – test data	0.926	0.896	0.904
Maxent Python Elapid	Checkerboard Cross-validation AUC score (test data with samples’ geographic weights)	0.882	0.862	0.868
Maxent Python Elapid	Model accuracy	0.935	0.911	0.920
Maxent Python Elapid	Misclassification rate	0.065	0.089	0.080

* The term “naïve” refers to a basic measure of a model’s ability to distinguish between positive and negative instances, with higher AUC values indicating better performance.

Table 3. Variables contribution to species spatial dispersal MaxEnt Version 3.4.4.

<i>Alexandrium</i> spp.		<i>L. polyedra</i>		<i>P. hartmanii</i>	
Variable	Percent contribution (%)	Variable	Percent contribution (%)	Variable	Percent contribution (%)
mean_NO ₃	78.3	mean_NO ₃	78.5	mean_NO ₃	64.3
mean_temp	10.2	mean_temp	7.8	mean_sal	27.3
mean_PO ₄	5.3	mean_sal	6.5	mean_PO ₄	5.4
mean_sal	3.0	mean_PO ₄	4.6	mean_temp	2.7
mean_pH	1.6	mean_DO	1.2	mean_pH	0.1
currents_speed	0.8	mean_ChI	1.0	currents_speed	0.1
mean_ChI	0.6	mean_pH	0.3	mean_ChI	0
mean_DO	0.3	currents_speed	0.2	mean_DO	0

Buoyancy frequency (N^2), Turner angle (Tu) and stability ratio (R_p) were obtained to address the specifics of the hydrodynamic conditions over the latitudinal gradient in the studied region. The calculations were performed at pressure midpoints ranging from a depth of -5.005 m to -2001.135 m, covering the latitudinal gradient of the Black Sea region based on mean annual datasets (potential temperature and practical salinity) obtained by CMEMS for three years: 2011, 2013, and 2015 (only the results for 2013 are presented).

High positive buoyancy frequency values indicate stable stratification and minimal vertical mixing, while lower positive N^2 values indicate a gradual change in density with depth (Monin 1990; McWilliams 2006), which can lead to weaker stratification and increased vertical mixing in the upper layer (0–25m), coinciding with the average mixed layer thickness (Fig. 3) over the latitudinal gradient in the spatial range confined within 41–45N. Low to moderate values of N^2 (evident in the latitudinal range from 45–46N) imply a moderate level of stratification, with a balance between stability and vertical mixing, suggesting specific water column dynamics in the north-western region. Furthermore, lower to moderate levels correspond to conditions promoting vertical exchanges in the water column, resulting in more effective nutrient transfer and increased biological production in the top layer.

The Turner angle reveals shifts in the orientation of water velocity at depths near 50 meters (Fig. 4), potentially impacting the patterns of horizontal transport. The values of the stability ratio (R_p) (Fig. 5) showed unstable stratification, implying a potential for vertical mixing and overturning of water masses at the surface to depths of 50 meters. A stability ratio of 0 is a precise point denoting a neutral state (Monin 1990; McWilliams 2006; Traxler et al. 2011), and the

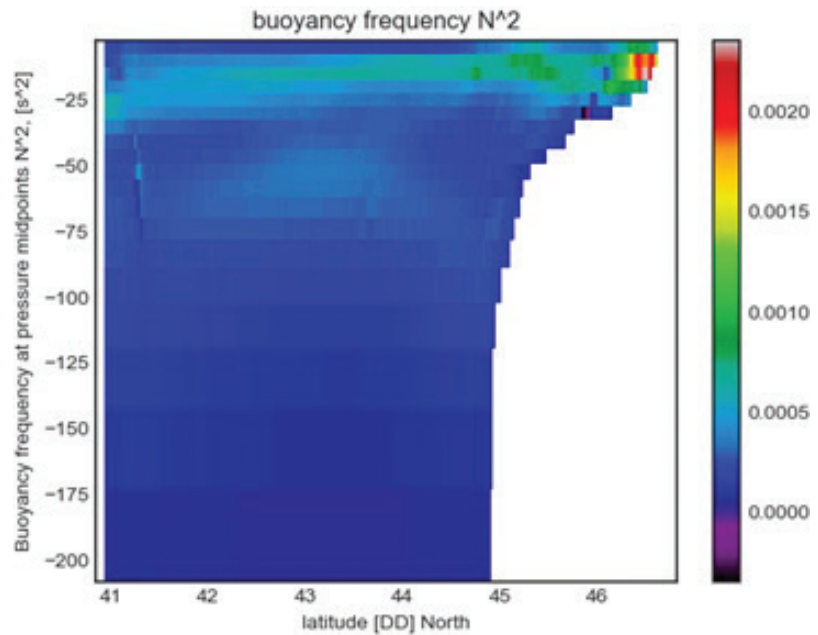


Figure 3. The buoyancy frequency (N), estimated using the Gibbs SeaWater (GSW) Oceanographic Toolbox of TEOS-10 (IOC, SCOR, and IAPSO 2010) implementation for Python.

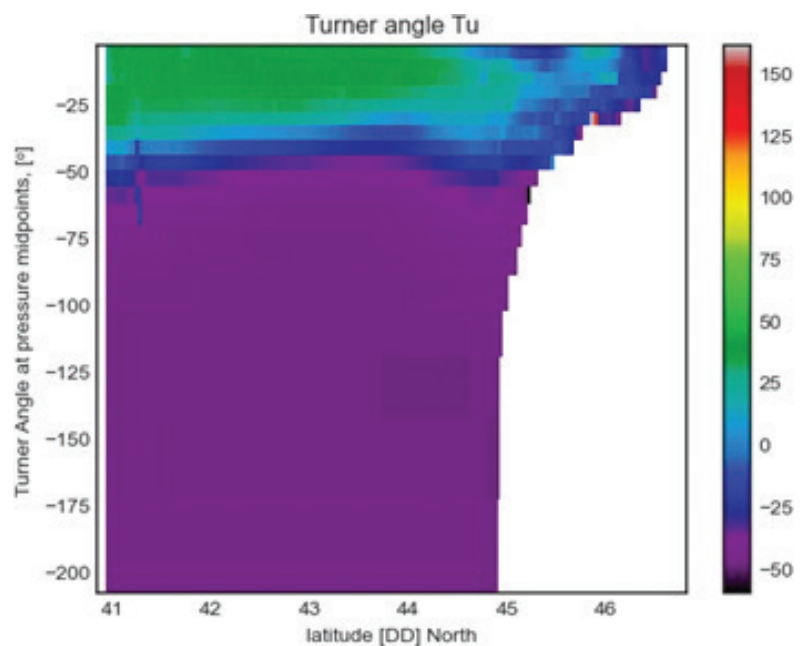


Figure 4. The Turner angle (Tu), estimated using the Gibbs SeaWater (GSW) Oceanographic Toolbox of TEOS-10 (IOC, SCOR, and IAPSO 2010) implementation for Python.

behavior of the water column will be influenced by the entirety of the oceanographic conditions in the area.

The combined effect of stability and stratification patterns in the water column is expected to affect the settling, vertical distribution, and horizontal transportation of cysts. The presence of a strong stratification can result in the formation of stable layers that facilitate the accumulation of cysts. Moreover, changes in the water mass flow direction, as indicated by the Turner angle, can affect the horizontal dispersal of cysts.

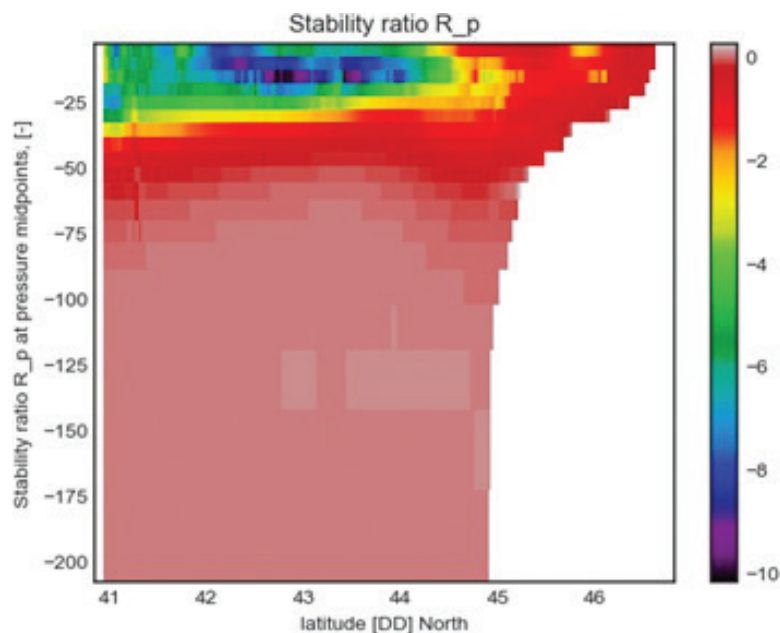


Figure 5. The stability ratio (R_p), estimated using the Gibbs SeaWater (GSW) Oceanographic Toolbox of TEOS-10 (IOC, SCOR, and IAPSO 2010) implementation for Python.

Discussion

Knowledge regarding the spatial dispersal, abundance, and diversity of cyst assemblages holds significant value in accurately evaluating phytoplankton biodiversity. It aids in comprehending how it is associated with biological, physical, and chemical oceanographic conditions of the surface water, identifying hot spot areas where resting cysts accumulate (cyst banks), and predicting potential harmful algal blooms (Genovesi-Giunti et al. 2006; Anderson et al. 2014; Mudie et al. 2017). This study provides a valuable supplement to the extensive mapping of dinoflagellate cysts in the surface sediment of the Black Sea (Mudie et al. 2017). It contributes new information regarding the occurrence, distribution, and abundance of 65 different taxa of dinoflagellate cysts, covering 27 species that were not previously documented in the Atlas, including 6 dormant forms of *Chaetoceros* diatoms (Table 1).

The presence of a large number of recorded cyst species confirms that Black Sea sediments have the ability to sustain significant biodiversity (Mudie et al. 2017). The Ukrainian coastal stations had the highest diversity indices (Suppl. material 1: table S3), which aligns with the abundance of phytoplankton species documented in this region (Moncheva et al. 2019). Peaks in total cyst concentration were observed in some samples, primarily due to the dominance of particular taxa (mainly *Scrippsiella* and *Chaetoceros*). The resting spores of *Chaetoceros* were both abundant and broadly distributed in the samples collected in the current research. The findings align with molecular data, which indicated that the genus has been among the most abundant and diverse taxa (Dzhembekova et al. 2018). Similar tendencies have been observed in other areas where seed banks were similarly characterized by predominant resting stages of *Chaetoceros* (Montresor et al. 2013; Casabianca et al. 2020). The seed banks of *Chaetoceros* spp. ensure their survival in unfavorable conditions (Pelusi et al. 2020) and enhance their ability to sustain the planktonic population in the water (Itakura et al. 1997; Ishikawa

and Furuya 2004). Confirming these findings, *Chaetoceros* spp. are among the most dominant species in the plankton community in the Black Sea, often forming blooms (Nesterova et al. 2008; Moncheva et al. 2019). Resting stage formation appeared to be an advantageous strategy for other dominant cyst species, such as *Scrippsiella acuminata*, to dominate both sediment assemblages and plankton communities in the Black Sea (Dzhenbekova et al. 2022a, and references therein). In contrast, certain species (*Pentaparsodinium tyrrhenicum*, *Pentaparsodinium dalei*, and *Calciodinellum albatrosianum*) that were present in the sediment samples are rarely observed or documented in the plankton of the Black Sea (Kra-khmalnyi et al. 2018). The latter demonstrates the benefits of conducting cyst surveys for detecting rare species, hence uncovering the 'hidden flora' in the basin (Persson et al. 2000; Godhe et al. 2001). Previously, there has been a documented disparity between the species that were dominant in the sediment's cyst assemblages and the typical members of the plankton community in the water column (Persson et al. 2000; Godhe et al. 2001; Rubino and Belmonte 2021). The latter can be attributed to several factors: a limited number of species that produce resting stages (McQuoid and Hobson 1996; Bravo and Figueroa 2014); many species spend longer periods resting in the sediment compared to the water column (Godhe and McQuoid 2003); there is a temporal and spatial mismatch between the occurrence of vegetative cell blooms and resting stage peaks, which can be caused by horizontal transfer in the water column or bioturbational mixing (Kirn et al. 2005; Ribeiro and Amorim 2008; Balkis et al. 2016); and incomplete inventories. Nevertheless, the benthic seed banks provide substantial genetic diversity and likelihood for survival, making a considerable contribution to the long-term viability of species that produce dormant stages (Lundholm et al. 2011, 2017).

Eight cyst taxa of potentially toxic dinoflagellates were identified in this study (Table 1). Despite the fact that the majority of them had a low concentration and a limited spread, *Lingulodinium polyedra*, *Alexandrium* spp., and *Polykrikos hartmannii* exhibited a higher likelihood of influencing bloom dynamics. The interaction between benthic cyst assemblages and pelagic active stages (one aspect of the benthic-pelagic coupling) is critical in encystment and excystment cycles, connecting blooms and subsequent cyst abundance, and vice versa (Anderson et al. 2014; Ishikawa et al. 2014). Sediment seed banks not only serve as historical records of past bloom occurrences, but they also signal a specific basin's future productivity potential and could be used to forecast forthcoming bloom events (Rubino et al. 2000; Anderson et al. 2014).

On a global scale, the dinoflagellate genus *Alexandrium* is one of the foremost harmful algal bloom-causing genera in terms of diversity, scale, and impact of blooms (Anderson et al. 2012). In this study, the genus *Alexandrium* was represented by a total of five determined and eight unidentified species (Table 1, Suppl. material 1: table S2), which exhibited variations in their morphology and size. In order to gain a more comprehensive understanding of the spread of the genus, *Alexandrium* cysts were combined and referred to as *Alexandrium* spp., due to the challenges associated with species identification. Several taxa were found to coexist in sediment samples in both the current and previous studies (Aydin et al. 2015; Mudie et al. 2017) and also in plankton samples (Dzhenbekova et al. 2022b). Although *Alexandrium* spp. often do not occur in large abundances, blooms of *A. monilatum* and *A. ostenfeldii* have been documented (Moncheva et al. 2001; Mavrodieva et al. 2007). The occurrence of

toxins linked to *Alexandrium* species has been recorded in the Black Sea, albeit at low concentrations (Vershinin et al. 2006; Kalinova 2015; Peteva et al. 2019).

Polykrikos hartmannii cysts, another potentially harmful dinoflagellate widely distributed in the Black Sea (Mudie et al. 2017), as well as identified in the plankton community with the application of a molecular approach (Dzhebekova et al. 2022b), were detected in 40% of the samples, encompassing all specified locations (Table 1, Suppl. material 1: table S2). The highest abundances were registered in samples collected from the western region of the basin. Although there have been no reports of blooms at the regional level, bloom densities and ichthyotoxicity have been observed in a brackish estuary (Tang et al. 2013).

The potentially toxic dinoflagellate *Lingulodinium polyedra* was found to be widely distributed and abundant in the sediments of the Black Sea, as shown in both the current study (Table 1, Suppl. material 1: table S2) and prior research (Nikonova 2010; Aydin et al. 2015; Mudie et al. 2017). It is also prevalent in phytoplankton communities (Moncheva et al. 2019). A significant correlation has been discovered between the abundance of *Lingulodinium polyedra* cells and the presence of yessotoxins (YTXs) in the Black Sea, thereby substantiating the ability of local strains to produce toxins (Dzhebekova et al. 2022b). The latter emphasizes further the significance of delineating regions that represent the highest environmental suitability to serve as cyst beds.

The results of our study indicate that the distribution of *Lingulodinium polyedra* cysts relative probability of occurrence in terms of suitable habitat is significantly influenced by nitrates and temperature. The key variables controlling the habitat suitability of *Alexandrium* spp. were nitrates and temperature, while for the *Polykrikos hartmannii* cysts, the main factors were nitrates and salinity (Table 3). The availability of nutrients, temperature, and salinity are typically regarded as the primary triggers for the encystment processes (Genovesi-Giunti et al. 2006 and references therein). Comparable findings were documented for other basins (Godhe and McQuoid 2003). The formation of resting cysts is a proven survival strategy employed by *L. polyedra* in response to adverse environmental conditions, such as nitrogen depletion and fluctuations in temperature (Ganini et al. 2013). The region with the highest likelihood of *L. polyedra* cyst occurrence appears to be in the western coastal and shelf waters (Fig. 2A), which includes areas where *L. polyedra* red tides have been documented (Terenko and Krakhmalnyi 2021 and references therein). The projected habitat suitability of the other studied taxa, *Alexandrium* spp. and *Polykrikos hartmannii* (Fig. 2B–C), partly coincided with the modeled distribution of *L. polyedra* cysts, likely due to the coexistence of the three genera and their shared preferences for environmental conditions, productivity, and survival strategies. Additionally, local hydrodynamic conditions and the transportation of cysts before their settlement in sediments could also contribute to this overlap.

Understanding the interplay among the water column dynamics, the sedimentation processes, and cyst settling is essential for investigating the ecology and life cycles of organisms that form cysts. The latter necessitates the evaluation of various elements, including water column stability, currents, mixing patterns, and the properties of the sediments. In general, the density of the water column plays a role in the larger environmental context that affects how cyst assemblages are distributed in the aquatic sediments (Nehring 1993; Harland et al. 2004; Genovesi-Giunti et al. 2006; Ribeiro and Amorim 2008).

Moreover, the overall hydrodynamic processes and sediments' characteristics have been indicated as having a major impact on cyst concentrations in the sediments (Ribeiro and Amorim 2008; Li et al. 2019; García-Moreiras et al. 2021). The vertical stability of the water column, which is advantageous for many dinoflagellate species, has been recognized as a pivotal factor affecting the seasonal variations in cyst production (Harland et al. 2004; Ribeiro and Amorim 2008). Additionally, the density of the water column might impact the sedimentation rates, therefore influencing the distribution of cysts (Cho and Matsuoka 2001). A water column with a lower density may undergo more intense vertical mixing. The process of mixing can impact the dispersion of particles, such as cysts, throughout the water column prior to their final settlement into sediments. Therefore, areas with minimal water current velocities exhibited higher cyst densities (Azanza et al. 2004). Considering the distinct vertical structure of the Black Sea (Oguz et al. 2000; Yakushev et al. 2008; Capet et al. 2016; Kaiser et al. 2017; Zatsepin and Podymov 2021), our findings can be concisely stated as follows: The water column exhibits unstable stratification in the upper layer (0 to 25 m, coinciding partly with the mixed layer depth thickness) along the latitudinal gradient, potentially influencing the vertical distribution of water properties and the settling of organisms, including cysts. The fluctuations in buoyancy frequency (N^2) indicate alterations in the intensity of stratification, exhibiting a prominent maximum at a depth close to 25–35 meters (the average thermocline layer depth) (Fig. 3). The Turner angle reveals shifts in the density gradients and the orientation of water velocity at depths near 50 meters in the latitudinal range from 45–46N (Fig. 4), potentially impacting the patterns of horizontal transport. Furthermore, riverine freshwater input plays a significant role in influencing the Western Black Sea by creating stratification and nutrient gradients, having further impact on the primary production, abundance, and composition of phytoplankton communities, including cyst-forming species (Moncheva et al. 2019; Dzhembekova et al. 2022a). The latter is related to the significant nutrient input (including nitrogen and phosphorus), the transportation of sediments (cysts, being relatively heavy, can settle in these sediments), and the sedimentation process, which can influence the spatial distribution of cysts along the river's plumes and in the adjacent Black Sea region.

The distribution of cysts is also significantly affected by sediment composition (Cho and Matsuoka 2001). Dinoflagellate cysts, due to their similar mass and hydrodynamic properties, are often distributed and deposited in sediment alongside fine-grained particles (Godhe and McQuoid 2003; Rachman et al. 2022), and generally higher concentrations of dinoflagellate cysts are observed in muddy sediments than in sandy sediments (Cho and Matsuoka 2001; Anderson 2023). Consistent with these findings, the area in the Western region of the Black Sea exhibiting the highest habitat suitability > 80% (at depths 50–100 m) is primarily represented by mixed sediments (shelly mud) for all modeled species (Suppl. material 1: table S7).

The north-western region of the Black Sea was identified as the most favorable habitat for the examined potentially toxic species (Fig. 2), posing a greater risk for the onset of algal blooms. Furthermore, this region aligns with predicted zones of very high risk of mass outbreaks of potentially toxic dinoflagellate *Prorocentrum cordatum* in the Black Sea (Goncharenko et al. 2021). Considering the aforementioned results, the identified hotspots provide potential inocu-

lum for bloom initiation (seed banks) and a suitable environment for vegetative growth and mass development of toxic dinoflagellates in the water column.

In conclusion, the accumulation of cysts pertains to how they are dispersed/transported within the water column from one location to another before settlement in sediment, whereas habitat suitability refers to the specific environmental conditions required for their survival, growth, and germination. Cysts can be dispersed in aquatic ecosystems by water currents, facilitating their colonization of new habitats. Both aspects, particularly the autoecology of the species and their life cycle, are crucial factors to comprehend when studying organisms that undergo cyst formation. However, the problem of modeling habitat suitability becomes challenging due to the spatial dispersal caused by horizontal transportation. This is because the specimens that have been sampled and documented as occurrences may have reached areas that are unsuitable or novel areas that could be suitable through horizontal transportation in a highly stratified environment. Therefore, model validation (Fig. 2, Table 2) is essential for accurately identifying suitable habitat and understanding the prospective transportation patterns associated with the local water column hydrodynamic properties and unique characteristics of the environment.

Additional information

Conflict of interest

The authors have declared that no competing interests exist.

Ethical statement

No ethical statement was reported.

Funding

This study was supported by the National Science Fund, Ministry of Education and Science (MES), Bulgaria, under the project "Phytoplankton cysts: an intricacy between a "memory" or a "potential" for Black Sea biodiversity and algal blooms" (Grant number DN01/8, 16.12.2016) and by the Contract No D01-164/28.07.2022 (project "National Geoinformation Center (NGIC)" financed by the Ministry of Education and Sciences of Bulgaria through the National Roadmap for Scientific Infrastructure 2020–2027.

Author contributions

Conceptualization: SM, ND, IZ. Organization of samplings: SM. Sediment treatment and analysis of cysts: FR, MB. Environmental data: IZ, IP, VD. Statistical analysis: IZ. Visualization: IP, IZ, VD, ND. Model evaluation and validation: IZ. Writing: original draft: ND, IZ, SM. Writing - review and editing: ND, IZ, FR, MB, VD, IP, SM. All authors contributed to the final version of the manuscript and approved the submitted version.

Author ORCIDs

Nina Dzhembekova  <https://orcid.org/0000-0001-9620-6422>


Ivelina Zlateva  <https://orcid.org/0000-0003-4133-5627>

Fernando Rubino  <https://orcid.org/0000-0003-2552-2510>

Manuela Belmonte  <https://orcid.org/0000-0001-6668-6920>

Valentina Doncheva  <https://orcid.org/0000-0002-6397-3024>

Ivan Popov  <https://orcid.org/0000-0002-2012-3628>

Snejana Moncheva  <https://orcid.org/0000-0002-4213-2111>

Data availability

All of the data that support the findings of this study are available in the main text or Supplementary Information.

References

- Anderson CB (2023) elapid: Species distribution modeling tools for Python. *Journal of Open Source Software* 8(84): 4930. <https://doi.org/10.21105/joss.04930>
- Anderson DM, Alpermann TJ, Cembella AD, Collos Y, Masseret E, Montresor M (2012) The globally distributed genus *Alexandrium*: Multifaceted roles in marine ecosystems and impacts on human health. *Harmful Algae* 14: 10–35. <https://doi.org/10.1016/j.hal.2011.10.012>
- Anderson DM, Keafer BA, Kleindinst JL, McGillicuddy Jr DJ, Martin JL, Norton K, Pilskaln CH, Smith JL, Sherwood CR, Butman B (2014) *Alexandrium fundyense* cysts in the Gulf of Maine: Long-term time series of abundance and distribution, and linkages to past and future blooms. *Deep-sea Research. Part II, Topical Studies in Oceanography* 103: 6–26. <https://doi.org/10.1016/j.dsr2.2013.10.002>
- Ari N, Ustazhanov M (2014) Matplotlib in python. In: 2014 11th International Conference on Electronics, Computer and Computation (ICECCO). IEEE, Abuja, Nigeria, 1–6. <https://doi.org/10.1109/ICECCO.2014.6997585>
- Aydin H, Balci M, Uzar S, Balkis-Ozdelice N (2015) Dinoflagellate cyst assemblages in surface sediments of southwestern Black Sea and Çanakkale strait (Dardanelles). *Fresenius Environmental Bulletin* 24: 4789–4798. <https://hdl.handle.net/20.500.12885/1334>
- Azanza RV, Siringan FP, Diego-Mcglone MLS, Yñiguez AT, Macalalad NH, Zamora PB, Agustin MB, Matsuoka K (2004) Horizontal dinoflagellate cyst distribution, sediment characteristics and benthic flux in Manila Bay, Philippines. *Phycological Research* 52(4): 376–386. <https://doi.org/10.1111/j.1440-183.2004.00355.x>
- Baldwin RA (2009) Use of Maximum Entropy Modeling in Wildlife Research. *Entropy (Basel, Switzerland)* 11(4): 854–866. <https://doi.org/10.3390/e11040854>
- Balkis N, Balci M, Giannakourou A, Venetsanopoulou A, Mudie P (2016) Dinoflagellate resting cysts in recent marine sediments from the Gulf of Gemlik (Marmara Sea, Turkey) and seasonal harmful algal blooms. *Phycologia* 55(2): 187–209. <https://doi.org/10.2216/15-93.1>
- Bekkar M, Djemaa H, Alitouche TA (2013) Evaluation Measures for Models Assessment over Imbalanced Data Sets. *Journal of Information Engineering and Applications*. <https://www.semanticscholar.org/paper/Evaluation-Measures-for-Models-Assessment-over-Data-Bekkar-Djemaa/bf6dec62269e5270d1588b1e893e9c2ac2214dea> [January 30, 2024]
- Belmonte G, Rubino F (2019) Resting Cysts from Coastal Marine Plankton. In: Hawkins SJ, Allcock AL, Bates AE, Firth LB, Smith IP, Swearer SE, Todd PA (Eds) *Oceanography and Marine Biology*. CRC Press, 1–88. <https://doi.org/10.1201/9780429026379-1>
- Bravo I, Figueroa R (2014) Towards an Ecological Understanding of Dinoflagellate Cyst Functions. *Microorganisms* 2(1): 11–32. <https://doi.org/10.3390/microorganisms2010011>
- Capet A, Meysman FJR, Akoumianaki I, Soetaert K, Grégoire M (2016) Integrating sediment biogeochemistry into 3D oceanic models: A study of benthic-pelagic coupling in the Black Sea. *Ocean Modelling (Oxford)* 101: 83–100. <https://doi.org/10.1016/j.ocemod.2016.03.006>

- Casabianca S, Capellacci S, Ricci F, Andreoni F, Russo T, Scardi M, Penna A (2020) Structure and environmental drivers of phytoplanktonic resting stage assemblages in the central Mediterranean Sea. *Marine Ecology Progress Series* 639: 73–89. <https://doi.org/10.3354/meps13244>
- Castañeda-Quezada R, García-Mendoza E, Ramírez-Mendoza R, Helenes J, Rivas D, Romo-Curiel AE, Lago-Lestón A (2021) Distribution of *Gymnodinium catenatum* Graham cysts and its relation to harmful algae blooms in the northern Gulf of California. *Journal of the Marine Biological Association of the United Kingdom* 101(6): 895–909. <https://doi.org/10.1017/S0025315421000795>
- Cayuela L, Golicher DJ, Newton AC, Kolb M, De Albuquerque FS, Arets EJMM, Alkemade JRM, Pérez AM (2009) Species Distribution Modeling in the Tropics: Problems, Potentialities, and the Role of Biological Data for Effective Species Conservation. *Tropical Conservation Science* 2(3): 319–352. <https://doi.org/10.1177/194008290900200304>
- Cho H-J, Matsuoka K (2001) Distribution of dinoflagellate cysts in surface sediments from the Yellow Sea and East China Sea. *Marine Micropaleontology* 42(3–4): 103–123. [https://doi.org/10.1016/S0377-8398\(01\)00016-0](https://doi.org/10.1016/S0377-8398(01)00016-0)
- Coops NC, Waring RH, Schroeder TA (2009) Combining a generic process-based productivity model and a statistical classification method to predict the presence and absence of tree species in the Pacific Northwest, U.S.A. *Ecological Modelling* 220(15): 1787–1796. <https://doi.org/10.1016/j.ecolmodel.2009.04.029>
- De Cáceres M, Jansen F (2016) Relationship between Species and Groups of Sites. Package ‘indicpecies’. <ftp://r-project.org/pub/R/web/packages/indicpecies/indicpecies.pdf>
- Dzhembekova N, Moncheva S, Ivanova P, Slabakova N, Nagai S (2018) Biodiversity of phytoplankton cyst assemblages in surface sediments of the Black Sea based on metabarcoding. *Biotechnology, Biotechnological Equipment* 32(6): 1507–1513. <https://doi.org/10.1080/13102818.2018.1532816>
- Dzhembekova N, Rubino F, Belmonte M, Zlateva I, Slabakova N, Ivanova P, Slabakova V, Nagai S, Moncheva S (2022a) Distribution of Different *Scrippsiella acuminata* (Dinophyta) Cyst Morphotypes in Surface Sediments of the Black Sea: A Basin Scale Approach. *Frontiers in Marine Science* 9: 864214. <https://doi.org/10.3389/fmars.2022.864214>
- Dzhembekova N, Moncheva S, Slabakova N, Zlateva I, Nagai S, Wietkamp S, Wellkamp M, Tillmann U, Krock B (2022b) New Knowledge on Distribution and Abundance of Toxic Microalgal Species and Related Toxins in the Northwestern Black Sea. *Toxins* 14(10): 685. <https://doi.org/10.3390/toxins14100685>
- Elith J, Leathwick JR (2009) Species Distribution Models: Ecological Explanation and Prediction Across Space and Time. *Annual Review of Ecology, Evolution, and Systematics* 40(1): 677–697. <https://doi.org/10.1146/annurev.ecolsys.110308.120159>
- Elith J, Phillips SJ, Hastie T, Dudík M, Chee YE, Yates CJ (2011) A statistical explanation of MaxEnt for ecologists: Statistical explanation of MaxEnt. *Diversity & Distributions* 17(1): 43–57. <https://doi.org/10.1111/j.1472-4642.2010.00725.x>
- Ellegaard M, Ribeiro S (2018) The long-term persistence of phytoplankton resting stages in aquatic ‘seed banks’. *Biological Reviews of the Cambridge Philosophical Society* 93(1): 166–183. <https://doi.org/10.1111/brv.12338>
- Feng X, Park DS, Walker C, Peterson AT, Merow C, Papeş M (2019) A checklist for maximizing reproducibility of ecological niche models. *Nature Ecology & Evolution* 3(10): 1382–1395. <https://doi.org/10.1038/s41559-019-0972-5>
- Fielding AH, Bell JF (1997) A review of methods for the assessment of prediction errors in conservation presence/absence models. *Environmental Conservation* 24(1): 38–49. <https://doi.org/10.1017/S0376892997000088>

- Ganini D, Hollnagel HC, Colepicolo P, Barros MP (2013) Hydrogen peroxide and nitric oxide trigger redox-related cyst formation in cultures of the dinoflagellate *Lingulodinium polyedrum*. *Harmful Algae* 27: 121–129. <https://doi.org/10.1016/j.hal.2013.05.002>
- García-Moreiras I, Oliveira A, Santos AI, Oliveira PB, Amorim A (2021) Environmental Factors Affecting Spatial Dinoflagellate Cyst Distribution in Surface Sediments Off Aveiro-Figueira da Foz (Atlantic Iberian Margin). *Frontiers in Marine Science* 8: 699483. <https://doi.org/10.3389/fmars.2021.699483>
- Genovesi-Giunti B, Laabir M, Vaquer A (2006) The benthic resting cyst: a key actor in harmful dinoflagellate blooms – a review. *Vie et Milieu / Life & Environment* 56: 327–337. <https://hal.sorbonne-universite.fr/hal-03228775>
- Gillies S (2013) The Shapely user manual. <https://pypi.org/project/Shapely>
- Gillies S (2019) Rasterio documentation. MapBox: San Francisco, CA, USA.
- Godhe A, McQuoid M (2003) Influence of benthic and pelagic environmental factors on the distribution of dinoflagellate cysts in surface sediments along the Swedish west coast. *Aquatic Microbial Ecology* 32: 185–201. <https://doi.org/10.3354/ame032185>
- Godhe A, Norén F, Kuylenshierna M, Ekberg C, Karlson B (2001) Relationship between planktonic dinoflagellate abundance, cysts recovered in sediment traps and environmental factors in the Gullmar Fjord, Sweden. *Journal of Plankton Research* 23(9): 923–938. <https://doi.org/10.1093/plankt/23.9.923>
- Goncharenko I, Krakhmalnyi M, Velikova V, Ascencio E, Krakhmalnyi A (2021) Ecological niche modeling of toxic dinoflagellate *Prorocentrum cordatum* in the Black Sea. *Ecohydrology & Hydrobiology* 21(4): 747–759. <https://doi.org/10.1016/j.ecohyd.2021.05.002>
- Grégoire M, Soetaert K (2010) Carbon, nitrogen, oxygen and sulfide budgets in the Black Sea: A biogeochemical model of the whole water column coupling the oxic and anoxic parts. *Ecological Modelling* 221(19): 2287–2301. <https://doi.org/10.1016/j.ecolmodel.2010.06.007>
- Grégoire M, Raick C, Soetaert K (2008) Numerical modeling of the central Black Sea ecosystem functioning during the eutrophication phase. *Progress in Oceanography*, 76(3): 286–333. <https://doi.org/10.1016/j.pocean.2008.01.002>
- Grégoire M, Vandenbulcke L, Capet A (2020) Black Sea Biogeochemical Reanalysis (CMEMS BS-Biogeochemistry): BLKSEA_REANALYSIS_BIO_007_005. Copernicus Monitoring Environment Marine Service (CMEMS). https://doi.org/10.25423/CMCC/BLKSEA_REANALYSIS_BIO_007_005_BAMHBI
- Guisan A, Thuiller W (2005) Predicting species distribution: Offering more than simple habitat models. *Ecology Letters* 8(9): 993–1009. <https://doi.org/10.1111/j.1461-0248.2005.00792.x>
- Hallegraeff GM (1993) A review of harmful algal blooms and their apparent global increase. *Phycologia* 32(2): 79–99. <https://doi.org/10.2216/i0031-8884-32-2-79.1>
- Harland R, Nordberg K, Filipsson HL (2004) The seasonal occurrence of dinoflagellate cysts in surface sediments from Koljö Fjord, west coast of Sweden – a note. *Review of Palaeobotany and Palynology* 128(1–2): 107–117. [https://doi.org/10.1016/S0034-6667\(03\)00115-5](https://doi.org/10.1016/S0034-6667(03)00115-5)
- Harris CR, Millman KJ, Van Der Walt SJ, Gommers R, Virtanen P, Cournapeau D, Wieser E, Taylor J, Berg S, Smith NJ, Kern R, Picus M, Hoyer S, Van Kerkwijk MH, Brett M, Haldane A, Del Río JF, Wiebe M, Peterson P, Gérard-Marchant P, Sheppard K, Reddy T, Weckesser W, Abbasi H, Gohlke C, Oliphant TE (2020) Array programming with NumPy. *Nature* 585(7825): 357–362. <https://doi.org/10.1038/s41586-020-2649-2>
- Holder AM, Markarian A, Doyle JM, Olson JR (2020) Predicting geographic distributions of fishes in remote stream networks using maximum entropy modeling and landscape

- characterizations. *Ecological Modelling* 433: 109231. <https://doi.org/10.1016/j.ecolmodel.2020.109231>
- Hossin M, Sulaiman MN (2015) A Review on Evaluation Metrics for Data Classification Evaluations. *International Journal of Data Mining & Knowledge Management Process* 5: 01–11. <https://doi.org/10.5121/ijdkp.2015.5201>
- Hoyer S, Hamman J (2017) xarray: N-D labeled Arrays and Datasets in Python. 5: 10. <https://doi.org/10.5334/jors.148>
- IOC SCOR and IAPSO (2010) The international thermodynamic equation of seawater – 2010: Calculation and use of thermodynamic properties. Intergovernmental Oceanographic Commission, Manuals and Guides No. 56, UNESCO (English), 196 pp. <https://unesdoc.unesco.org/ark:/48223/pf0000188170>
- Ishikawa A, Furuya K (2004) The role of diatom resting stages in the onset of the spring bloom in the East China Sea. *Marine Biology* 145(3): 633–639. <https://doi.org/10.1007/s00227-004-1331-9>
- Ishikawa A, Hattori M, Ishii K-I, Kulis DM, Anderson DM, Imai I (2014) In situ dynamics of cyst and vegetative cell populations of the toxic dinoflagellate *Alexandrium catenella* in Ago Bay, central Japan. *Journal of Plankton Research* 36(5): 1333–1343. <https://doi.org/10.1093/plankt/fbu048>
- Itakura S, Imai I, Itoh K (1997) “Seed bank” of coastal planktonic diatoms in bottom sediments of Hiroshima Bay, Seto Inland Sea, Japan. *Marine Biology* 128(3): 497–508. <https://doi.org/10.1007/s002270050116>
- Jordahl K, Bossche JVD, Fleischmann M, Wasserman J, McBride J, Gerard J, Tratner J, Perry M, Badaracco AG, Farmer C, Hjelle GA, Snow AD, Cochran M, Gillies S, Culbertson L, Bartos M, Eubank N, Maxalbert, Bilogur A, Rey S, Ren C, Arribas-Bel D, Wasser L, Wolf LJ, Journois M, Wilson J, Greenhall A, Holdgraf C, Filipe, Leblanc F (2020) *geopandas/geopandas: v0.8.1*. <https://doi.org/10.5281/ZENODO.3946761>
- Kaiser D, Konovalov S, Schulz-Bull DE, Waniek JJ (2017) Organic matter along longitudinal and vertical gradients in the Black Sea. *Deep-sea Research. Part I, Oceanographic Research Papers* 129: 22–31. <https://doi.org/10.1016/j.dsr.2017.09.006>
- Kalinova G (2015) A study of paralytic toxins in cultured mussels from Bulgarian Black Sea. *Trakia Journal of Sciences* 13(Suppl.2): 303–308. <https://doi.org/10.15547/tjs.2015.s.02.065>
- Kindt R, Kindt MR (2019) Package ‘BiodiversityR’. Package for community ecology and suitability analysis, 2, 11–12.
- Kirn SL, Townsend DW, Pettigrew NR (2005) Suspended *Alexandrium* spp. hypnozygote cysts in the Gulf of Maine. *Deep-sea Research. Part II, Topical Studies in Oceanography* 52(19–21): 2543–2559. <https://doi.org/10.1016/j.dsr2.2005.06.009>
- Kluyver T, Ragan-Kelley B, Pérez F, Granger B, Bussonnier M, Frederic J, Kelley K, Hamrick J, Grout J, Corlay S, Ivanov P, Avila D, Abdalla S, Willing C Jupyter development team (2016) Jupyter Notebooks – a publishing format for reproducible computational workflows. In: Loizides F, Schmidt B (Eds) IOS Press, 87–90. <https://doi.org/10.3233/978-1-61499-649-1-87>
- Krakhmalnyi AF, Okolodkov YB, Bryantseva YuV, Sergeeva AV, Velikova VN, Derezyuk NV, Terenko GV, Kostenko AG, Krakhmalnyi MA (2018) Revision of the dinoflagellate species composition of the Black Sea. *Algologia* 28(4): 428–448. <https://doi.org/10.15407/alg28.04.428>
- Kremp A, Rengefors K, Montresor M (2009) Species specific encystment patterns in three Baltic cold-water dinoflagellates: The role of multiple cues in resting cyst formation. *Limnology and Oceanography* 54(4): 1125–1138. <https://doi.org/10.4319/lo.2009.54.4.1125>

- Kremp A, Hinners J, Klais R, Leppänen A-P, Kallio A (2018) Patterns of vertical cyst distribution and survival in 100-year-old sediment archives of three spring dinoflagellate species from the Northern Baltic Sea. *European Journal of Phycology* 53(2): 135–145. <https://doi.org/10.1080/09670262.2017.1386330>
- Li Y, Tang Y-N, Shen P-P, Li G, Tan Y-H (2019) Distribution of harmful dinoflagellate cysts in the surface sediments of Daya Bay of the South China Sea and their relationship to environmental factors. *International Biodeterioration & Biodegradation* 139: 44–53. <https://doi.org/10.1016/j.ibiod.2019.02.006>
- Lima L, Aydogdu A, Escudier R, Masina S, Ciliberti SA, Azevedo D, Peneva EL, Causio S, Cipollone A, Clementi E, Cretí S, Stefanizzi L, Lecci R, Palermo F, Coppini G, Pinardi N, Palazov A (2020) Black Sea Physical Reanalysis (CMEMS BS-Currents) (Version 1) [Data set]. Copernicus Monitoring Environment Marine Service (CMEMS). https://doi.org/10.25423/CMCC/BLKSEA_MULTIYEAR_PHY_007_004
- Lundholm N, Ribeiro S, Andersen TJ, Koch T, Godhe A, Ekelund F, Ellegaard M (2011) Buried alive – germination of up to a century-old marine protist resting stages. *Phycologia* 50(6): 629–640. <https://doi.org/10.2216/11-16.1>
- Lundholm N, Ribeiro S, Godhe A, Rostgaard Nielsen L, Ellegaard M (2017) Exploring the impact of multidecadal environmental changes on the population genetic structure of a marine primary producer. *Ecology and Evolution* 7(9): 3132–3142. <https://doi.org/10.1002/ece3.2906>
- Mamun M, Kim S, An K-G (2018) Distribution pattern prediction of an invasive alien species largemouth bass using a maximum entropy model (MaxEnt) in the Korean peninsula. *Journal of Asia-Pacific Biodiversity* 11(4): 516–524. <https://doi.org/10.1016/j.japb.2018.09.007>
- Mavrodieva R, Moncheva S, Hiebaum G (2007) Abnormal outburst of the dinoflagellate *Alexandrium ostenfeldii* (Paulsen) Balech et Tangen along the Bulgarian Black sea coast (the bay of Sozopol) in winter - ecological surprise or ecological concern? In: *Bdua Journal of Biology*.
- McDougall TJ, Barker PM (2011) Getting started with TEOS-10 and the Gibbs Seawater (GSW) Oceanographic Toolbox. SCOR/IAPSO WG127. https://www.teos-10.org/pubs/Getting_Started.pdf
- McKinney W (2010) Data Structures for Statistical Computing in Python. In: Austin, Texas, 56–61. <https://doi.org/10.25080/Majora-92bf1922-00a>
- McQuoid MR, Hobson LA (1996) Diatom resting stages. *Journal of Phycology* 32(6): 889–902. <https://doi.org/10.1111/j.0022-3646.1996.00889.x>
- McWilliams JC (2006) Fundamentals of geophysical fluid dynamics. First paperback ed. (with corr.). Cambridge University Press, Cambridge, 249 pp.
- Moncheva S, Gotsis-Skretas O, Pagou K, Krastev A (2001) Phytoplankton Blooms in Black Sea and Mediterranean Coastal Ecosystems Subjected to Anthropogenic Eutrophication: Similarities and Differences. *Estuarine, Coastal and Shelf Science* 53(3): 281–295. <https://doi.org/10.1006/ecss.2001.0767>
- Moncheva S, Boicenco L, Mikaelyan AS, Zotov A, Dereziuk N, Gvarishvili C, Slabakova N, Mavrodieva R, Vlas O, Pautova LA, Silkin VA, Medinets V, Sahin F, Feyzioglu AM (2019) Phytoplankton. In: *State of the Environment of the Black Sea (2009–2014/5)*. Publications of the Commission on the Protection of the Black Sea Against Pollution (BSC). Istanbul, Turkey, 225–285. <http://www.blacksea-commission.org/SoE2009-2014/SoE2009-2014.pdf>
- Monin AS (1990) Theoretical geophysical fluid dynamics. Kluwer Academic Publishers, Dordrecht, Boston, 399 pp. <https://doi.org/10.1007/978-94-009-1880-1>

- Montresor M, Bastianini M, Cucchiari E, Giacobbe M, Penna A, Rubino F, Satta CT (2010) Capitolo 26. Stadi Di Resistenza Del Plankton. In: Metodologie Di Studio Del Plancton Marino. Manuali e Linee Guida 56. Rome: ISPRA - Istituto Superiore per la protezione e la ricerca ambientale, 258–273. https://www.isprambiente.gov.it/files/pubblicazioni/manuali-lineeguida/9171_MLG56_2010.pdf
- Montresor M, Di Prisco C, Sarno D, Margiotta F, Zingone A (2013) Diversity and germination patterns of diatom resting stages at a coastal Mediterranean site. *Marine Ecology Progress Series* 484: 79–95. <https://doi.org/10.3354/meps10236>
- Mudie PJ, Marret F, Mertens KN, Shumilovskikh L, Leroy SAG (2017) Atlas of modern dinoflagellate cyst distributions in the Black Sea Corridor: From Aegean to Aral Seas, including Marmara, Black, Azov and Caspian Seas. *Marine Micropaleontology* 134: 1–152. <https://doi.org/10.1016/j.marmicro.2017.05.004>
- Muscarella R, Galante PJ, Soley-Guardia M, Boria RA, Kass JM, Uriarte M, Anderson RP (2014) ENMeval: An R package for conducting spatially independent evaluations and estimating optimal model complexity for Maxent ecological niche models. *Methods in Ecology and Evolution* 5(11): 1198–1205. <https://doi.org/10.1111/2041-210X.12261>
- Nehring S (1993) Mechanisms for recurrent nuisance algal blooms in coastal zones: resting cyst formation as life-strategy of dinoflagellates. In: Proceedings of the International Coastal Congress, ICC-Kiel '92: Interdisciplinary Discussion of Coastal Research and Coastal Management Issues and Problems. P. Lang, Frankfurt, 454–467.
- Nesterova D, Moncheva S, Mikaelyan A, Vershinin A, Akatov V, Boicenco L, Aktan Y, Sahin F, Gvarishvili T (2008) Chapter 5. The State of Phytoplankton. In: State of the Environment of the Black Sea (2001–2006/7). In: BSC, 2008. State of the Environment of the Black Sea (2001–2006/7). Black Sea Commission Publications 2008-3, Istanbul, Turkey, 419 pp.
- Nikonova S (2010) Dinoflagellate Cysts of Odessa and Tendra Regions of the Northwestern Part of the Black Sea. *Scientific Issue Ternopil Volodymyr Hnatiuk National Pedagogical University Series: Biology* 3: 190–192.
- Oguz T, Ducklow HW, Malanotte-Rizzoli P (2000) Modeling distinct vertical biogeochemical structure of the Black Sea: Dynamical coupling of the oxic, suboxic, and anoxic layers. *Global Biogeochemical Cycles* 14(4): 1331–1352. <https://doi.org/10.1029/1999GB001253>
- Pearson RG, Phillips SJ, Lorant MM, Beck PSA, Damoulas T, Knight SJ, Goetz SJ (2013) Shifts in Arctic vegetation and associated feedbacks under climate change. *Nature Climate Change* 3(7): 673–677. <https://doi.org/10.1038/nclimate1858>
- Pedregosa F, Varoquaux G, Gramfort A, Michel V, Thirion B, Grisel O, Blondel M, Prettenhofer P, Weiss R, Dubourg V, Vanderplas J, Passos A, Cournapeau D, Brucher M, Perrot M, Duchesnay É (2011) Scikit-learn: Machine Learning in Python. *Journal of Machine Learning Research* 12: 2825–2830. <http://jmlr.org/papers/v12/pedregosa11a.html> [January 30, 2024]
- Pelusi A, Santelia ME, Benvenuto G, Godhe A, Montresor M (2020) The diatom *Chaetoceros socialis*: Spore formation and preservation. *European Journal of Phycology* 55(1): 1–10. <https://doi.org/10.1080/09670262.2019.1632935>
- Persson A, Godhe A, Karlson B (2000) Dinoflagellate Cysts in Recent Sediments from the West Coast of Sweden. *Botanica Marina* 43(1). <https://doi.org/10.1515/BOT.2000.006>
- Peterson A, Soberón J, Pearson R, Anderson R, Martínez-Meyer E, Nakamura M, Araújo M (2012) *Ecological Niches and Geographic Distributions* (MPB-49). Publisher: Princeton University Press. <https://doi.org/10.1515/9781400840670>

- Peteva ZV, Kalinova GN, Krock B, Stancheva MD, Georgieva SK (2019) Evaluation of paralytic shellfish poisoning toxin profile of mussels from Bulgarian North Black Sea coast by HPLC-FID with post and pre-column derivatization. *Izvestia po Himiia* 51: 233–240. https://epic.awi.de/id/eprint/55941/1/Peteva_2019.pdf
- Phillips SJ, Anderson RP, Schapire RE (2006) Maximum entropy modeling of species geographic distributions. *Ecological Modelling* 190(3–4): 231–259. <https://doi.org/10.1016/j.ecolmodel.2005.03.026>
- Phillips SJ, Anderson RP, Dudík M, Schapire RE, Blair ME (2017) Opening the black box: An open-source release of Maxent. *Ecography* 40(7): 887–893. <https://doi.org/10.1111/ecog.03049>
- Picoche C, Barraquand F (2022) Seed banks can help to maintain the diversity of interacting phytoplankton species. *Journal of Theoretical Biology* 538: 111020. <https://doi.org/10.1016/j.jtbi.2022.111020>
- Pospelova V, Chmura GL, Walker HA (2004) Environmental factors influencing the spatial distribution of dinoflagellate cyst assemblages in shallow lagoons of southern New England (USA). *Review of Palaeobotany and Palynology* 128(1–2): 7–34. [https://doi.org/10.1016/S0034-6667\(03\)00110-6](https://doi.org/10.1016/S0034-6667(03)00110-6)
- Ptaczniak R, Solimini AG, Andersen T, Tamminen T, Brettum P, Lepistö L, Willén E, Rekolainen S (2008) Diversity predicts stability and resource use efficiency in natural phytoplankton communities. *Proceedings of the National Academy of Sciences of the United States of America* 105(13): 5134–5138. <https://doi.org/10.1073/pnas.0708328105>
- QGIS Development Team (2009) “QGIS Geographic Information System.”, v.3.34. [Online]. <http://qgis.org>
- R Core Team (2022) R: A Language and Environment for Statistical Computing. <https://www.R-project.org>
- Rachman A, Thoha H, Intan MDB, Sianturi OR, Witasari Y, Wibowo SPA, Iwataki M (2022) Dinoflagellate Cyst Distribution in Relation to the Sediment Composition and Grain Size in the Coastal Area of Pangkajene, South Sulawesi, Indonesia. *Ilmu Kelautan: Indonesian Journal of Marine Sciences* 27(2): 111–123. <https://doi.org/10.14710/ik.ijms.27.2.111-123>
- Ribeiro S, Amorim A (2008) Environmental drivers of temporal succession in recent dinoflagellate cyst assemblages from a coastal site in the North-East Atlantic (Lisbon Bay, Portugal). *Marine Micropaleontology* 68(1–2): 156–178. <https://doi.org/10.1016/j.marmicro.2008.01.013>
- Richter D, Vink A, Zonneveld KAF, Kuhlmann H, Willems H (2007) Calcareous dinoflagellate cyst distributions in surface sediments from upwelling areas off NW Africa, and their relationships with environmental parameters of the upper water column. *Marine Micropaleontology* 63(3–4): 201–228. <https://doi.org/10.1016/j.marmicro.2006.12.002>
- Roquet F, Madec G, McDougall TJ, Barker PM (2015) Accurate polynomial expressions for the density and specific volume of seawater using the TEOS-10 standard. *Ocean Modelling (Oxford)* 90: 29–43. <https://doi.org/10.1016/j.ocemod.2015.04.002>
- Rubino F, Belmonte G (2021) Habitat Shift for Plankton: The Living Side of Benthic-Pelagic Coupling in the Mar Piccolo of Taranto (Southern Italy, Ionian Sea). *Water (Basel)* 13(24): 3619. <https://doi.org/10.3390/w13243619>
- Rubino F, Belmonte G, Miglietta AM, Geraci S, Boero F (2000) Resting Stages of Plankton in Recent North Adriatic Sediments. *Marine Ecology (Berlin)* 21(3–4): 263–284. <https://doi.org/10.1046/j.1439-0485.2000.00725.x>
- Sgrosso S, Esposito F, Montresor M (2001) Temperature and daylength regulate encystment in calcareous cyst-forming dinoflagellates. *Marine Ecology Progress Series* 211: 77–87. <https://doi.org/10.3354/meps211077>

- Shin HH, Li Z, Lim D, Lee K-W, Seo MH, Lim WA (2018) Seasonal production of dinoflagellate cysts in relation to environmental characteristics in Jinhae-Masan Bay, Korea: One-year sediment trap observation. *Estuarine, Coastal and Shelf Science* 215: 83–93. <https://doi.org/10.1016/j.ecss.2018.09.031>
- Smith A, Page B, Duffy K, Slotow R (2012) Using Maximum Entropy modeling to predict the potential distributions of large trees for conservation planning. *Ecosphere* 3(6): 1–21. <https://doi.org/10.1890/ES12-00053.1>
- Tang YZ, Harke MJ, Gobler CJ (2013) Morphology, phylogeny, dynamics, and ichthyotoxicity of *Pheopolykrikos hartmannii* (Dinophyceae) isolates and blooms from New York, USA. Cock M (Ed.). *Journal of Phycology* 49: 1084–1094. <https://doi.org/10.1111/jpy.12114>
- Terenko G, Krakhmalnyi A (2021) Red tide of the *Lingulodinium polyedrum* (Dinophyceae) in Odessa Bay (Black Sea). *Turkish Journal of Fisheries and Aquatic Sciences* 22(4): TRJFAS20312. <https://doi.org/10.4194/TRJFAS20312>
- Thyng K, Greene C, Hetland R, Zimmerle H, DiMarco S (2016) True Colors of Oceanography: Guidelines for Effective and Accurate Colormap Selection. *Oceanography* (Washington, D.C.) 29(3): 9–13. <https://doi.org/10.5670/oceanog.2016.66>
- Traxler A, Stellmach S, Garaud P, Radko T, Brummell N (2011) Dynamics of fingering convection. Part 1 Small-scale fluxes and large-scale instabilities. *Journal of Fluid Mechanics* 677: 530–553. <https://doi.org/10.1017/jfm.2011.98>
- Urbani F, D'Alessandro P, Frasca R, Biondi M (2015) Maximum entropy modeling of geographic distributions of the flea beetle species endemic in Italy (Coleoptera: Chrysomelidae: Galerucinae: Alticini). *Zoologischer Anzeiger* 258: 99–109. <https://doi.org/10.1016/j.jcz.2015.08.002>
- Van Rossum G, Drake Jr FL (1995) Python tutorial. <https://ir.cwi.nl/pub/5007/05007D.pdf>
- Vasquez M, Allen H, Manca E, Castle L, Lillis H, Agnesi S, Al Hamdani Z, Annunziatellis A, Askew N, Bekkby T, Bentes L, Doncheva V, Drakopoulou V, Duncan G, Gonçalves J, Inghilesi R, Laamanen L, Loukaidi V, Martin S, McGrath F, Mo G, Monteiro P, Muresan M, Nikilova C, O'Keeffe E, Pesch R, Pinder J, Populus J, Ridgeway A, Sakellariou D, Teaca A, Tempera F, Todorova V, Tunesi L, Virtanen E (2021) EUSeaMap 2021. A European broad-scale seabed habitat map. EMODnet. <https://doi.org/10.13155/83528>
- Vershinin A, Morton S, Leighfield T, Pankov S, Smith L, Quilliam M, Ramsdell J (2006) *Alexandrium* in the Black Sea – identity, ecology and PSP toxicity. *African Journal of Marine Science* 28(2): 209–213. <https://doi.org/10.2989/18142320609504149>
- Wang R, Li Q, He S, Liu Y, Wang M, Jiang G (2018) Modeling and mapping the current and future distribution of *Pseudomonas syringae* pv. *actinidiae* under climate change in China. Arnold DL (Ed.). *PLoS ONE* 13: e0192153. <https://doi.org/10.1371/journal.pone.0192153>
- White EP, Thibault KM, Xiao X (2012) Characterizing species abundance distributions across taxa and ecosystems using a simple maximum entropy model. *Ecology* 93(8): 1772–1778. <https://doi.org/10.1890/11-2177.1>
- WoRMS Editorial Board (2023) World Register of Marine Species. <https://www.marine-species.org> at VLIZ. [Accessed 2023-11-16] <https://doi.org/10.14284/170>
- Yakushev EV, Chasovnikov VK, Murray JW, Pakhomova SV, Podymov OI, Stunzhas PA (2008) Vertical Hydrochemical Structure of the Black Sea. In: Kostianoy AG, Kosarev AN (Eds) *The Black Sea Environment. The Handbook of Environmental Chemistry*. Springer, Berlin, Heidelberg, 277–307. https://doi.org/10.1007/698_5_088
- Yan H, Feng L, Zhao Y, Feng L, Wu D, Zhu C (2020) Prediction of the spatial distribution of *Alternanthera philoxeroides* in China based on ArcGIS and MaxEnt. *Global Ecology and Conservation* 21: e00856. <https://doi.org/10.1016/j.gecco.2019.e00856>

- Yost AC, Petersen SL, Gregg M, Miller R (2008) Predictive modeling and mapping sage grouse (*Centrocercus urophasianus*) nesting habitat using Maximum Entropy and a long-term dataset from Southern Oregon. *Ecological Informatics* 3(6): 375–386. <https://doi.org/10.1016/j.ecoinf.2008.08.004>
- Zatsepin AG, Podymov OI (2021) Thermohaline Anomalies and Fronts in the Black Sea and Their Relationship with the Vertical Fine Structure. *Oceanology, Academy of Sciences of the USSR* 61(6): 757–768. <https://doi.org/10.1134/S0001437021060321>
- Zonneveld KAF, Marret F, Versteegh GJM, Bogus K, Bonnet S, Bouimtarhan I, Crouch E, de Vernal A, Elshanawany R, Edwards L, Esper O, Forke S, Grøsfjeld K, Henry M, Holzwarth U, Kiehl J-F, Kim S-Y, Ladouceur S, Ledu D, Chen L, Limoges A, Londeix L, Lu S-H, Mahmoud MS, Marino G, Matsouka K, Matthiessen J, Mildenhall DC, Mudie P, Neil HL, Pospelova V, Qi Y, Radi T, Richerol T, Rochon A, Sangiorgi F, Solignac S, Turon J-L, Verleye T, Wang Y, Wang Z, Young M (2013) Atlas of modern dinoflagellate cyst distribution based on 2405 data points. *Review of Palaeobotany and Palynology* 191: 1–197. <https://doi.org/10.1016/j.revpalbo.2012.08.003>

Supplementary material 1

Supplementary information

Authors: Nina Dzhenbekova, Ivelina Zlateva, Fernando Rubino, Manuela Belmonte, Valentina Doncheva, Ivan Popov, Snezana Moncheva

Data type: docx

Explanation note: **table S1**. Sampling stations (location, sampling date, geographic coordinates, depth). **table S2**. Range of the cysts species concentration (cysts g⁻¹) per different geographic locations. In the table the different cyst types unidentified at the species level were first combined as spp. (marked in grey) and below the different taxa were listed (* potentially toxic species; + species not reported in Mudie et al. 2017). **table S3**. Diversity indices. **table S4**. Species diversity per sediment type (only the sediment types where species have been sampled was included in the analysis). **table S5**. Indicator species analysis – species association to sediment type. **table S6**. Indicator species analysis – species association indices (indices for assessing the strength of association between species and groups of sites) to geographic area (BG – Bulgaria; GE – Georgia; RO – Romania; TR – Turkey; UA – Ukraine), with bold are marked the species with association to sites $Indval > 0.5$. **table S7**. Sediment types for habitat suitability > 80% (relative probability of occurrence > 0.8) for *Polykrikos hartmanii*, *Lingulodinium polyedra*, and *Alexandrium* spp. **fig. S1**. MaxEnt Version 3.4.4 gridded outputs in terms of Habitat suitability maps of A) *Alexandrium* spp. B) *L. polyedra* C) *P. hartmanii* in the Black Sea coastal and shelf waters (represented with a colour scheme, with light blue indicating the least likelihood of suitable conditions, light orange – indicating conditions equal to those where species were found, and purple corresponding to the highest predicted probability of suitable environment).

Copyright notice: This dataset is made available under the Open Database License (<http://opendatacommons.org/licenses/odbl/1.0/>). The Open Database License (ODbL) is a license agreement intended to allow users to freely share, modify, and use this Dataset while maintaining this same freedom for others, provided that the original source and author(s) are credited.

Link: <https://doi.org/10.3897/natureconservation.55.121181.suppl1>